Mag. pharm. Verena Wahl

Modification of dry powder inhaler carrier surfaces by wet decantation

Characterization and improvement of the decantation process

MASTERARBEIT

for obtaining the academic degree of

Diplom – Ingenieurin

Masterstudium Chemical and Pharmaceutical Engineering

submittet to

Technischen Universität Graz

Advisor:

Univ. – Prof. Dipl. –Ing. Dr.techn. Johannes Khinast

Institute for Process and Particle Engineering, Technische Universität, Graz

Co – Advisor:

Annalisa Mercuri, PhD

Research Center Pharmaceutical Engineering GmbH, Graz

Graz, Oktober 2014

Acknowledgements

First of all, I want to thank Johannes Khinast for the opportunity to accomplish my master thesis under his supervision and to give me the opportunity to do this thesis in the field of pharmaceutical engineering.

I would like to sincerely thank Annalisa Mercuri for her support.

Moreover, my gratitude goes to Marcos Llusa, Milica Stankovic and Sharareh Salar – Behzadi.

Further thanks go to the laboratory team of the RCPE for the companionship and support during the whole study. Additionally, I would like to thank Hartmuth Schröttner for providing the SEM images.

Very special thanks go to Piet who helped and supported me.

Finally, my greatest thanks go to my family, who enabled me this study.

EIDESSTATTLICHE ERKLÄRUNG

AFFIDAVIT

Ich erkläre an Eides Statt, dass ich die vorliegende Arbeit selbstständig verfasst, andere als die angegebene Quellen/Hilfsmittel nicht benutzt, und die den benutzen Quellen wörtlich und inhaltlich entnommenen Stellen als solche kenntlich gemacht habe. Das TUGRAZonline hochgeladene Textdokument ist mit der vorliegenden Masterarbeit identisch.

I declare that I have authored this thesis independently, that I have not used other than the declared sources/resources, and that I have explicitly indicated all material which has been quoted either literally or by content from the sources used. The text document uploaded to TUGRAZonline is identical to the present master's thesis.

Datum / Date	Unterschrift /Signature

ABSTRACT

Ensuring development and manufacture of effective, reliable and robust drug products is a major objective of pharmaceutical companies. Over recent years it has became clear that inhalation products, and specifically dry powder inhaler (DPI) formulations, present multiple challenges during development in order to achieve this goal. In this work we focused on the modification of a dry powder inhaler carrier. Through decantation processes the surface was "cleaned" by removing the carrier fine particles adhering at the surface.

In a first step an appropriate method for determining the particle size as well as the particle size distribution was developed. To do so, dry dispersion methods as well as wet dispersion experiments were performed. Afterwards, a wet decantation process was performed with a 1 kg lactose carrier batch. The material before and after the decantation process was analyzed according to solid state, particle size, water content, specific surface area and roughness. Additionally, a stability study according to ICH guidelines was performed and the lactose carrier was exposed to accelerated storage conditions. It was observed that the engineered carrier was stable according to several particle attributes. In a last step an improvement study of the wet decantation process was implemented. Therefore, critical process parameters were identified. After performing the experiments, the influence of these parameters on the process was analyzed. We were able to identify a significant influencing factor, namely the number of cycles of the decantation process.

KURZFASSUNG

Um die Effektivität und Robustheit von Trockenpulverinhalatoren zu gewährleisten ist es nötig die Beladung des Trägermaterial mit Wirkstoff sicherzustellen. Eine besonders wichtige Rolle spielen hierbei die Interaktionen zwischen Partikeln, wobei dem Feinpartikelanteil im Trägermaterial besondere Bedeutung zukommt. Das Ziel dieser Diplomarbeit ist die Entfernung des Feinpartikelanteils mittels Dekantierung um die Oberfläche des Trägermaterials (Laktose) zu modifizieren und damit die Formulierung von Trockenpulverinhalatoren zu verbessern. Um den Erfolg des Prozesses zu überprüfen, wurden unter Anwendung verschiedener Methoden (u.a. REM (Rasterelektronenmikroskopie), Partikelgrößenverteilung, Oberflächenrauheit) sowohl das Ausgangsmaterial als auch das prozessierte Produkt charakterisiert.

Zu Beginn der Studie wurde eine Methode zur Bestimmung der Partikelgröße bzw. Partikelgrößenverteilung entwickelt. Im Anschluss wurde ein 1 kg Batch Laktoseträgermaterial nass dekantiert und charakterisiert, sowie eine einmonatige Stabilitätsstudie nach ICH (International Conference on Harmonization) Richtlinien durchgeführt. Zuletzt wurde ein Design of experiment (DoE) aufgestellt um den angewendeten Dekantierungs - Prozess zu verbessern. Dafür wurden kritische Prozessparameter identifiziert und nach Durchführung der Versuche evaluiert. Die Anzahl der durchgeführten Dekantierungszyklen wurde als signifikanter Faktor identifiziert.

Table of contents

List of tables

List of figures

List of equations

Abbreviations

Å	Angstrom
AD	After decantation
AIF	Angle of internal friction
API	Active pharmaceutical ingredient
AR	Aspect ratio
BD	Before decantation
BET	Brunnauer – Emmet - Teller
BFE	Basic flow energy
BJH	Barrett, Joyner, Halenda
CI	Carr index
CV	Convexity
DOE	Design of experiments
DPI	Dry powder inhaler
DSC	Differential scanning calorimetry
ff_c	Flow function
F_{max}	Ferets diameter maximum
F_{min}	Ferets diameter minimum
FTIR	Fourier – Transformed infrared spectroscopy
HR	Hausner ratio
ICH	International Conference on Harmonization
K	Kelvin
MDI	Metered dose inhaler
PEQC	Perimeter of the equivalent diameter

Ph. Eur.	European Pharmacopeia
PSD	Particle size distribution
RH	Relative humidity
RI	Refractive index
Rq	Root mean square
S	Sphericity
SAXS	Small angle X – ray scattering
SD	Standard deviation
Sec	Seconds
SEM	Scanning electron microscopy
TGA	Thermogravimetric analysis
V_0	Apparent volume
V_{500}	Tapped volume
WAXS	Wide angle X – ray scattering
σ_1	consolidation stress
σ_c	yield stress

1. Introduction

1.1 Pulmonary drug delivery

Over the last years the use of drugs via the pulmonary route is steadily increased and it is now accepted as being the optimal route of administration to treat respiratory diseases. Inhaled medications have been available on the market for the treatment of lung diseases such as asthma, since many years. Furthermore, inhalation drugs can be used as systemic drug delivery for the treatment of extrapulmonary diseases. More recently, research has focused on the delivering of biomolecules such as peptides and proteins via the pulmonary route to the systemic circulation due to the large absorptive surface area of the respiratory system (an adult offers a surface of approximately 100 m^2 which behaves like a highly permeable membrane) (1,2).

Pulmonary drug delivery offers various advantages compared to other administration routes. Via the lung, the drug is able to reach the blood stream avoiding the digestive system and the liver. Therefore, barriers like the first–pass effect and poor gastrointestinal absorption can be avoided. Additionally, it is possible to achieve a similar or superior therapeutic effect at a fraction of a dose given systemically as a local treatment is provided. Thus, less side effects compared to systematic treatment are given. The inhaled pharmaceutical dosage form provides a noninvasive “needle–free” delivery system (3).

1.2 Dry powder inhalers (DPI)

Three different types of inhaler devices have been used in the last years; these are defined as nebulizers, metered dose inhalers (MDI) and dry powder inhalers (DPI). Nebulizers use oxygen, compressed air or ultrasonic power to break up solutions or suspensions to small aerosol droplets which can be directly inhaled. These devices are widely used for the treatment of hospitalized or non – ambulatory patients as nebulizers are often too big to be used as portable devices, but also portable nebulizers are on the market. The drug is present in a solution or a suspension which is converted into a fine aerosol by compressed air or ultrasound and it is then inhaled by the patient (4).

The most widely used device for the treatment of respiratory tract diseases is the pressurized metered dose inhaler (MDI), which uses a propellant gas to expel droplets containing the pharmaceutical product. However, the MDI contain chlorofluorocarbons, and therefore, for environmental reasons, the use of MDIs is disadvantageous (4).

Dry powder inhalers (DPIs) offer a good alternative to metered dose inhalers. In DPIs, the active pharmaceutical ingredient (API) is present as dry powder loaded into an inert carrier and the aerosolization is triggered just by human breath (5). Upon aerolization, the API powder formulation must deaggregate from the carrier into fine drug particles, which have to be in the 1-5 µm range for effective pulmonary delivery (6).

The DPIs carrier material ensures flowability, reduces agglomeration and provides bulk to make handling and dosing possible (7). However, the delivery of dry powder particles of pharmaceutical products into the respiratory tract presents some issues. In fact, the inhaler should deliver the maximum possible proportion of the active particles to the lungs, including a significant proportion to the lower lung, preferably at the low inhalation capabilities since some patient, especially asthmatics, may have impaired breathing (8).

The major advantages of DPIs in comparison to other devices and technologies are the stability of the drug substance, the wide range of dose weights that can be rapidly administered with one or just few inhalations, a potentially high lung deposition and a reduced need for the patient to coordinate firing with inhalation (9).

Two main properties have to be ensured for every inhaler to achieve the desired therapeutic effect. Initially a uniform dosage has to be guaranteed, which means that every actuation should release the same amount of API. Furthermore, a high respirable fraction of the inhalation powder must be provided that is able to deposit in the deeper parts of the lung. The deposition behaviour of a particle in the lung is determined by three main mechanisms, depending on the aerodynamic diameter and density of the particle, which are: impaction, sedimentation and diffusion. Due to its inertia, the aerosol particle is not able to follow the air stream and impacts on bifurcations of the lung airways. Sedimentation is the mechanism of deposition when the particle settles in the airways forced by gravity. Diffusion is the main mechanism of deposition for particles with a diameter lower than 1 µm, which interact with gas molecules due to Brownian motion within the air. API penetration in the deeper lung will only be achieved if the aerodynamic diameter of the API particles is below 5 µm. Larger particles tend, in fact, to impact in the mouth, throat and the upper airways, while particles smaller than 0.5 µm are likely to be exhaled.

As powders of 0.5 µm to 5 µm in diameter are very cohesive, they show poor flowability, poor dosing and insufficient aerolization behaviour after release from the inhaler, which further cause variability and low amount of API that reaches the deeper lung. Inadequate flowability and aerosolization are especially challenging in dry powder inhalers, where dosing is performed volumetrically by free flowing of the powder into an orifice and aerosolization is acheived without propellant. Recent studies have shown that the carrier morphology directly affects the aerolization from a DPI (10–12). The most important factors that affect dry powder inhalation are particle size, shape, density, stability, moisture, crystallinity (polymorphism and amorphous nature of the API), surface chemistry, area and texture, plasticity, and electrostatics of the components of the adhesive mixtures (8). Particle–particle interactions between drug and carrier particles are a surface phenomenon, mainly dependent upon physicochemical properties of the interacting particles such as the particle size, shape and surface texture as well as electrostatic properties and hygroscopicity. The probably most

important attribute influencing the performance of carrier particles is the surface topography (13). The interaction forces between drug and carrier surface are predominantly Van der Waals, followed by electrostatic forces and capillary forces. Therefore, the inter-particle forces have to be strong enough to form stable mixtures of API and carrier and to guarantee adequate dosing (14). According to inter particle forces different problems can arise in dry powder inhalers. Particle interaction between the drug and the carrier particles depends on the contact area between two distinct particles. Strong inter-particle forces between the drug and the carriers may prevent the separation of the micronized drug particle from the coarse carrier on inhalation, and as such, the availability of the drug to reach the respiratory tract is limited. These strong interactions between drug and carrier may occur within asperities and clefts on the carrier surface, as the latter provides highly energetic sites on which the active particles are preferably attracted to and strongly adhere (15).

Irregular surface structures prevent the particles from close interaction and ease the separation from each other upon aerodynamic stress. The decrease of roughness is believed to lead to larger contact areas compared to rough surfaces (16) and therefore to improve aerolization efficiency of a drug carrier blend (17). There are two mechanisms playing a role for the impact on the fine particle fraction. First, the fine carrier particles occupy the high energy and adhesion areas of the carrier surface reducing the amount of drug particles strongly bound to the carrier. Secondly, the adhesion of carrier fines modifies the surface roughness properties leading to less drug-carrier adhesion forces (16,18). Ternary formulation approaches, whereby a fraction of fine particles is added, has been applied to improve the DPI performance (19). Additionally, the surface free energy of the carrier has to be considered. The use of low surface free energy materials, such as magnesium stearate or leucine, has been reported as a possible mean of increasing the aerolization efficacy of such a system (15).

1.3 Carrier material

The carrier materials typically used in DPIs are sugars or sugar-alcohols like lactose, glucose or mannitol. Lactose is the most frequently used carrier in dry powder inhalation (20). There are many pharmaceutical grades of lactose, which differ in physical properties and flow characteristics, as spray dried or crystalline powders of α-lactose and β-lactose (21). Microscopically α-lactose monohydrate appears as pyramid and tomahawk shaped crystals. The carrier particles must have high crystallinity (11). Lactose mostly has small amorphous parts at the surface, which influences the compressibility of the powder (22). Lactose is soluble in 2.04 parts of water at 50°C (21). The advantages of lactose are the known toxicity profile, GRAS status, broad availability with low cost, low hygroscopicity (23) as well as smooth surfaces and regular shape, which lead to good flowability. Recent research has demonstrated that the critical attributes of lactose carrier for DPI include size, size

distribution, shape and surface roughness of the particles, as well as the presence of moisture, impurities or amorphous lactose content on the surface of the crystals. Additionally, the content of fine lactose (24) and the quality and source (25), as well as ternary additive particles (26), can be critical according to the efficiency of a powder formulation. Furthermore, aspects such as crystalline habit of the lactose and the presence of either fine lactose particles in powder formulation or ternary additives (i.e. magnesium stearate or leucine) have been investigated as along with the effect of lactose pre–treatment processes such as washing (9).

Some of the advantages of using lactose are the possibility to have adverse reactions due to lactose intolerance occurring in persons with deficiency of the intestinal enzyme lactase (27). Also, lactose has reducing properties and would not be the appropriate excipient for drugs which contain amminoacids such as proteins or peptides (10). Several studies on the use of lactose in dry powder inhalers can be found in the literature (10,25,28).

1.4 Motivation and aim of the work

The key for the successful development of a DPI product is the preparation of a formulation that can provide reproducible and acceptable powder flowability, dosing efficacy and delivery of the drug particulates to the respiratory system (29). Despite the fact that a lot of considerable research has been done on the role of lactose in adhesive mixtures used in dry powder inhalers, the relationship between the physicochemical properties of the lactose carrier in adhesive mixtures and the performance of the dry powder inhaler remains largely unclear. Thus, complex interactions between the components within a formulation are not well understood. The ability to control inter particulate forces (cohesion) would enable the development of formulations with a more reproducible fine particle dose. (9). From the literature it can be observed that the effect of fine carrier particles in the powder mixture has shown to improve drug deposition for a number of drugs, however, it is not clear how fine lactose particles influence drug dispersion (30,31).

The modification of lactose according to fine particles can be divided into three general areas:

- crystallization: lactose is crystallized from a lactose solution
- solution phase processing: lactose is exposed to a liquid media and does not completely dissolve so that partial dissolution or etching may occur
- dry processing: lactose is “treated”, i.e by co–processing in the absence of a liquid

These methodologies attempt to increase the aerolization of drug via geometric and morphological modifications (32). A decrease in lactose surface together with an optimal level of fines is said to result in an improved lactose carrier performance, which will be drug and device dependent (32).

Therefore, the aim of this work is to investigate the possibility to modify the surface characteristics of an inhalation carrier such as lactose. The increase of carrier smoothness can be obtained by removal of fine lactose particles using the process of wet decantation (16,31). The fines adherent to the coarse carrier can be removed via this process. In fact, lactose is only partially soluble in 96% ethanol, so the expectation is that fine particles can be removed by using this solvent (16). By repeated decantation, an increased amount of fine particles is removed, leaving the larger lactose particles with a smooth surface. Decreased roughness can expose the high energetic sites on the carrier surface either to the fine carrier particles or to the drug particles. Decantation can be obtained by consecutive dispersions of lactose coarse carrier particles in absolute ethanol to remove carrier fines, and addition of dichloromethane to prevent solid bridges between coarse carrier particles (16). Subsequently a well defined type and amount of carrier fines can be added to the decanted material, in order to tailor and optimize drug loading and the fine particle fraction.

This work focuses on the modification of a lactose carrier via decantation process and on the physico-chemical characterization the powder before and after the decantation process analysing various parameters. Since several variables can affect the success of the decantation process, the best combination of process parameters should be identified. Therefore, to optimize the decantation process, design of experiments (DOE) was implemented by firstly evaluating the critical process parameters and then include them into the experimental plan. Based on the DOE results an improvement of the decantation process is also described in this thesis.

2. Material and methods

2.1 Materials

A commercial available α-lactose monohydrate was used in this study. Ethanol absolute was obtained from Sigma Aldrich (Munich, Germany).

2.2 Wet decantation

Fine particles were removed from the α-lactose monohydrate by means of decantation. The material was decanted using absolute ethanol as medium; the process was repeated for certain numbers of times. Ethanol absolute was added to the powder, and the mixture was vigorously stirred to form a homogenous suspension, which was then allowed to settle for few minutes at ambient conditions. Sedimentation time was calculated from the Stokes equations:

$$v_s = \frac{2}{9} * \frac{\rho_p - \rho_f}{\mu} * g * R^2$$

Equation 1: Stokes equation; $v_s$is the particle's settling velocity (m/s), g is the gravitational acceleration (m/s2) ρ_p is the mass density of the particles (kg/m^3), ρ_f is the mass density of the fluid (kg/m^3) and μ is the dynamic viscosity (kg/m*s), R is the thermal velocity

$$t = \frac{h}{v_s}$$

Equation 2: Sedimentation time; t is the time (min), h is the height of the beaker (m) and v_s is the particle's settling velocity (m/s)

The cloudy supernatant suspension was decanted and replaced with fresh ethanol. During the removal of the supernatant, special care was taken to ensure minimum disturbance of the lower layer of the suspension. At the end of the decantation process, the powder sample was left to dry for 2–4 days under a fume hood and stored afterwards in desiccators containing silica.

2.3 Dynamic image analysis

The particle size distribution and particle shape were analysed by means of Qicpic System (OASIS wet and dry system, Sympatec GmbH, Clausthal-Zellerfeld, Germany). Millions of particles were investigated by the principle of dynamic image analysis. A dispersion pressure of 0.5 bar was used. Three measurements (n = 3) were taken using a sample size of approximately 4 g lactose powder for each measurement.

The QicPic uses rear illumination with a visible pulsed light source that has an exposure time of 1 ns to minimize motion blur. The flash rate of the light source is adjustable from 1 to 500 Hz, and is synchronized with the high-speed camera that operates up to 500 frames per second. Dry powders are fed into the high-speed dry-sample disperser where they are

accelerated to a speed of up to 100 m/s via a Venturi tube located in the dispersing line. During this process, dry powders are dispersed and aerosolized by particle–particle, particle–wall collisions and centrifugal forces caused by velocity gradients. Upon exit, particles enter the measurement zone decelerated and are finally collected by a Nilfisk™ vacuum system (Nilfisk-Advance A/S, Sognevej, Denmark). In a typical experiment, at least 50,000 images of the investigated particles are captured by the camera and processed using appropriate image analysis algorithms included in the Windox 5.6.0.0 software.

The median of the particle size distribution is defined as x_{50} and describes a particle diameter corresponding to 50 % of the cumulative undersize distribution.

The parameter S (sphericity) is defined as the ratio of the perimeter of the equivalent circle (PEQPC) to the real perimeter (P_{real}). The equivalent circle gives the smallest possible perimeter at a given projection area, and therefore the value of S ranges between 0 and 1. The smaller the value the more irregular is the shape.

The aspect ratio (AR) is the ratio of F_{min} (Feret's diameter minimum) to F_{max} (Feret's diameter maximum) and again it ranges between 0 and 1. It reflects the elongation of a particle and the deviation from a sphere. Convexity (CV) is the ratio of the projection area of a particle to the area of a convex hull, which is calculated from particle projection. It describes the compactness of a particle. The smaller the value the more concave region a particle has and vice versa.

2.4 Laser diffraction

2.4.1 HELOS

Particle size distribution of the carrier product was determined by laser diffraction (HELOS/KR, Sympatec GmbH, Clausthal-Zellerfeld, Germany) using both wet (Lixell wet dispersion cell, Sympatec, Clausthal-Zellerfeld, Germany) and dry dispersing unit (Rodos/L, Sympatec, Clausthal-Zellerfeld, Germany). For the dry dispersion a pressure of 0.5-5 bars was used for the measurements. For the wet dispersion the suspension was ultrasonicated for 20 sec before starting each measurement. The Mie theory was used for data evaluation including the refractive index (RI) of ethanol (1.36) and lactose (1.347). Measurements were performed in triplicate (n = 3) and the typical sampling time was 30 seconds. The software Windox 5.6.0.0 (Sympatec, Clausthal-Zellerfeld, Germany) was used for data evaluation.

The generated Q_3 and Q_0 distributions were normalized in Excel. The normalization of the fraction $Q_{r,i}$ to the size of the corresponding interval leads to the distribution density. The span of the particle size distribution was calculated the following:

$$\frac{x_{90} - x_{10}}{x_{50}}$$

Equation 3: Span of the particle size distribution; x10 is the 10th percentile of the particle size distribution, x50 is the 50th percentile of the particle size distribution, x90 is the 90th percentile of the particle size distribution

2.5 Mastersizer

The Mastersizer 2000 (Malvern Instruments Limited, Malvern, UK), which is utilized with a helium-neon laser as the light source, was used to determine the particle size of the lactose carrier. Measurements were performed in triplicates (n = 3). The dry dispersion unit was used by applying a dispersing pressure of 0.5 bar. Also the wet dispersion unit was used (stirrer speed = 1750; ultrasonic = 20 sec before each measurement). The lactose powder was dispersed in absolute ethanol, which has a refractive index (RI) of 1.36 and the real RI of Lactose is 1.347. The Mie theory was used for data evaluation. The typical sampling time was 6 seconds.

2.6 Scanning electron microscopy (SEM)

Lactose morphology was examined before and after decantation using a scanning electron microscope (SEM) (Zeiss Ultra 55, Zeiss, Oberkochen/Germany) operating at 5 kV. The lactose particles were sputtered with gold-palladium prior to analysis. The images were taken at FELMI (Austrian Center for Electron Microscopy and Nanoanalysis, Graz). From each sample 5-6 pictures were taken at different magnifications.

2.7 Specific surface area

The specific surface of the bulk powder was investigated using the Micromeritics Tristar II 3020 (Norcross,USA). The samples (n = 3) were degassed for two days at 60°C at the Micromeritics VacPrep 061 degas unit (Norcross,USA). The measurements were performed using nitrogen gas. Brunauer, Emmett, and Teller (BET) adsorption theory was used to calculate the specific surface areas, using a pressure range of 0.05–0.30 normalized to the saturation pressure of the adsorbate.

The method of Barrett, Joyner, and Halenda (BJH) was used for calculating pore size distributions from experimental isotherms using the Kelvin model of pore filling. It applies to the mesopore and small macropore size range.

2.8 Powder flow properties

2.8.1 Angle of repose (AoR)

The angle of repose was determined by using a glass cylinder as described in the US Pharmacopoeia (USP 2007, 1174). The lactose powder was placed in a glass funnel with a closable aperture (HWS Labortechnik, RTG DIN ISO 4.324), 2-4 cm above an underlying

glass plate with 10 cm diameter. The aperture was opened and the carrier flowed onto the glass plate until the glass was completely covered. By rotating an iron wire, stuck and fine particles were pushed through the glass funnel. Mounted with a scale, the height of the cone, formed by the carrier, was measured. By knowing the diameter and the height of the cone, the angle of repose could be calculated by the following equation:

$$\tan(\propto) = \arctan\left(\frac{h}{r}\right) * (\frac{180}{\pi})$$

Equation 4: Angle of repose; h is the height of the cone, r its diameter

2.8.2 Bulk and tapped density

The bulk and tap densities were analyzed using a dry, graduated, 100 mL cylinder (readable to 2 mL), according to standardized method (USP 2007, 1174). A known mass of powder was poured into the cylinder up to a certain level and the weight was recorded. The tapped density was calculated after mechanically tapping the powder sample. The bulk and tap densities are necessary to estimate the flow indexes (such as the Hausner ratio and Carr index).

2.8.3 Carr Index (CI) and Hausner Ratio (HR)

Carr´s Index of lactose samples was calculated from the apparent volumes (apparent V_0 and tapped volume V_{500}), using the method described in USP 2007. Carr's index was determined using following formula:

$$CI = 100 * \frac{V0 - V500}{V0}$$

Equation 5: Carr index; V_0 is the apparent volume; V_{500} is the tapped volume

The ratio between the tap density and apparent density of a powder mass defines the Hausner Ratio. It is provides useful indication of the cohesive characteristics of a powder.

2.8.4 Flow properties by FT4

The flow function (ffc) (a shear-based flow index) and the angle of internal friction (AIF) were measured in a 1 mL shear cell module of a powder rheometer (FT4 (Freeman Technology, Tewkesbury, UK)). It measures the shear stress, τ, at different values of normal stress, σ, to provide indication of how easily a powder will move from a static condition into dynamic flow (33).

Basic Flowability Energy (BFE) was also quantified with the FT4. BFE is defined as the energy required to establish a particular flow pattern in a conditioned, precise volume of powder.

2.9 Small and wide angle x – ray scattering (SWAXS)

Small- and wide angle x – ray (SWAXS) scatteringwas used to determine specific inner surface at the nanoscale (1-100 nm) and the crystallinity of the powder. SWAXS measurements were carried out at 20 ± 1°C in a S3 – MICRO camera (formerly Hecus X – ray systems, Graz, now Bruker AXS, Karlsruhe). Specific inner surface analysis was performed by SAXS according to Porod theory (34) involving the measurement of integral scattering power Q and decay coefficient k. Q is proportional to the sample volume, and k to the surface, hence the ratio k/Q is proportional to the specific surface ($Å^2$/ $Å^3$). In this case, any interface between domains of different density contributes to the scattering, including inaccessible pores, or areas of different molecular packing, e.g. crystalline vs. amorphous. Obviously the contrast between solid matter and air dominates the effect. Crystallinity was measured by WAXS in the angular range between 17 and 27°, corresponding to real space dimensions of 4.9 and 3.3 Å, where molecular crystals show strong diffraction peaks. To avoid preferential orientation effects of crystallites, the samples held in capillaries of 2 mm i.d. were rotated during measurement. Typical exposure times were 1200 sec and measurements were performed in triplicates.

2.10 Differential scanning calorimetry (DSC)

The lactose samples before and after decantation were characterized by a differential scanning calorimeter (DSC 204F1 Phoenix®, Netzsch GmbH, Selb, Germany). Samples of about 10-12 mg (n = 3) were weighed into aluminium pans, which were pierced. The samples were heated from 25 to 200 °C at a heating rate of 10 K/min using pure nitrogen as purging gas at a flow rate of 20 mL/min. After cooling at 10 K/min to 25 °C, a second heating run was performed. An empty aluminum pan was used as a reference. The DSC data analysis was conducted with Proteus Thermal Analysis software (Netzsch GmbH, Selb, Germany). The equipment was calibrated with adamantane, indium, bismuth, tin and zinc before the measurements.

2.11 Stability tests

To evaluate the physical and chemical stability of the carrier after decantation, the impact of temperature and humidity was studied. As from the ICH guidelines (35), the samples were stored for 38 days at accelerated conditions (40 ± 2°C / 75 ± 5% R.H.).

2.12 Attenuated reflectance – Fourier transformed – infrared spectroscopy (ATR – FTIR)

IR spectra were recorded on a Bruker VERTEX 70 (Bruker, Rheinstetten, Germany) apparatus using a DLaTGS detector and an ATR unit (MVP Pro Star, Diamond crystal). A total of 64 scans were performed at wavelengths ranging from 4000–600 cm^{-1} with a

resolution of 4 cm^{-1}. Three samples were collected from each batch and subjected to IR measurements.

2.13 Design of experiments (DOE)

A DOE (design of experiments) was designed using MODDE 9.1 (Umetrics, Umeå, Sweden) to check the influence and the interactions of different factors on the decantation process. The following factors were identified to have potential criticality for the process: the solvent/solid ratio, the mixing time and the number of cycles. Sedimentation time was kept constant for all experiments. The responses were defined, as the x_{50} and x_{10}, the surface roughness taken from SEM images and the BET surface of the decanted carrier. The data set contains the average value (n = 3) for each powder property. As several responses were measured, PLS (partial least square) was useful to fit a model simultaneously representing the variation of all responses to the variation of the factors, by taking their co-variances into account (36). PLS is a common chemometric data analytical tool, which has various implementations like correlating responses. Since experimental design has a high condition number or small amounts of missing data in the response matrix PLS is useful for data evaluation. The two-block predictive PLS version is the most widespread form in science and technology; it relates two data matrices, X (factors) and Y(responses) (Y-data are modeled by the X-data) via a linear multivariate model and it models the structure of X and Y (37). Models can be used to support design spaces across multiple scales and equipment (38).

3. Results and Discussion

The results and discussion Chapter is divided into three paragraphs. The first one is dealing with the implementation and improvement of the particle size analysis of unprocessed and processed α-lactose monohydrate. The second paragraph discusses the decantation of 1 kg batch of the carrier material using an in-house process and its characterization using several methods before and after processing. Additionally, a stability study was performed to verify the robustness of the processed lactose.

To improve the in-house decantation process and to define critical process parameters, a design of experiments (DOE) was performed. These results are discussed in the third paragraph of this Thesis.

3.1 Identifying a method for measuring the particle size and particle size distribution (PSD)

The particle size and particle size distribution are one of the most important product characteristics as, together with particle shape, many product properties can be determined by these properties. This relationship can be divided in the following three directions: properties for further processing, the quality of the process (in which particles are produced) and product properties related to a given application (39).

For inhalation powders, it has recently been found that the adhesion force between drug and carrier particles depends not only on the mean particle size of the carrier material (40), but also on the amount of fine lactose particles which are present in the formulation. It is practically impossible to absolutely classify particles in terms of particle size and distribution (32). Herein, particle size and particle size distribution measurements of the lactose carrier were used to investigate the decreasing amount of small particles after decantation in comparison to the starting material.

When processing the α-lactose monohydrate powder, the whole particle size distribution (PSD) of the batch was used. According to published data it has to be assumed that the particle size is not changing during decantation (31). As the focus of the PSD was set on the fine particle fraction (here: <15 µm), it was challenging to find the ideal way to investigate this certain powder fraction as several issues arised when measuring the PSD, as we the sample had a very broad particle size distribution (big particles and very particle very small). Often measurement and detection limitation can occur when determining the particle size (41). A broad particle size distribution is also called a polydisperse system. When the size differs by a factor of 10 or more, the difference in the surface of these particles has a difference of more than a factor of 100 and the volume and mass more than a factor of 1000. Therefore, narrow particle size distributions have better possibilities to show tiny differences in particle size than wide classes. (1). According to angular scattering patterns (which are insensitive to the particle size) the scattered intensity at any angle decreases so drastically with size that

contributions from fine particles are overwhelmed by those from coarser material (41). This is especially a problem when fine material needs to be measured. In our case, it was assumed that the amount of particles < 15 µm was decreasing after decantation, as they were removed by the process. Therefore, different methods and principles of determining the particle size distribution of the processed and unprocessed material were investigated, in order to determine the best method to describe this particular sample.

In a first experiment the principle of dynamic image analysis was used to measure the particle size distribution. From Table 1 and Figure 1, it can be observed that the particle size is decreasing after decantation and the span of the particle size distribution is increasing.

Table 1: Particle size before and after decantation (±sd) – Qicpic (0.5 bar dispersion pressure):

	x10[µm]	x50[µm]	x90[µm]	Span of particle size
Before decantation	147.1±1.42	262.1±1.43	350.5±0.75	0.78
After decantation	114.5±0.96	215.6±2.85	329.4±4.26	0.99

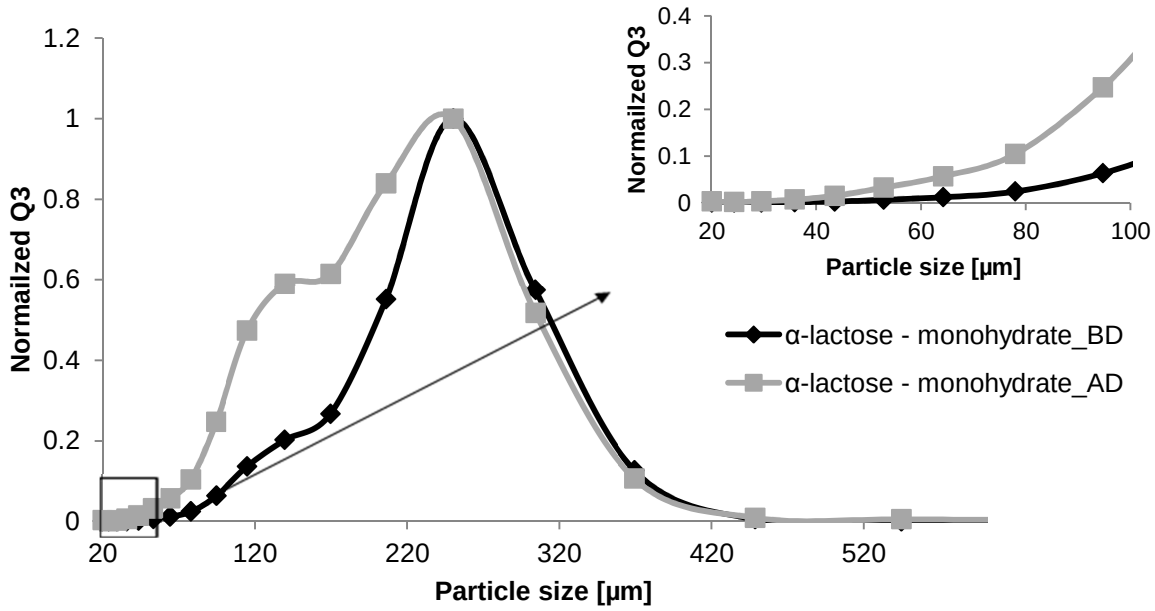

Figure 1: Normalized Q3 distribution of the carrier material - Qicpic (0.5 bar dispersion pressure) BD – Before decantation AD – After decantation

In Figure 1 it can be observed that the volume distribution of particles in the range of 20–100 µm is increasing after decantation. Also the Q3 distribution of particles in the range from 100–180 µm is increasing. According to Table 1, the particle size is decreasing of approximately 20%. The Q2 and the Q0 distribution can be found in Appendix 1. As the

Qicpic has only a sensitivity for particles > 20µm, we used in a next experiment the principle of laser diffraction to determine the particle size of the lactose carrier to account for the fines contribution to the PSD. Two different equipments were used for these investigations, namely the Helos (Sympatec GmbH) and the Mastersizer 2000 (Malvern). The powder was investigated with the Helos, under dry dispersion unit, using different dispersion pressures (0.5–5 bar) to identify the optimal experimental conditions to be used for the lactose powder. In Figure 2 it is shown the influence of the dispersion pressure on the particle size.

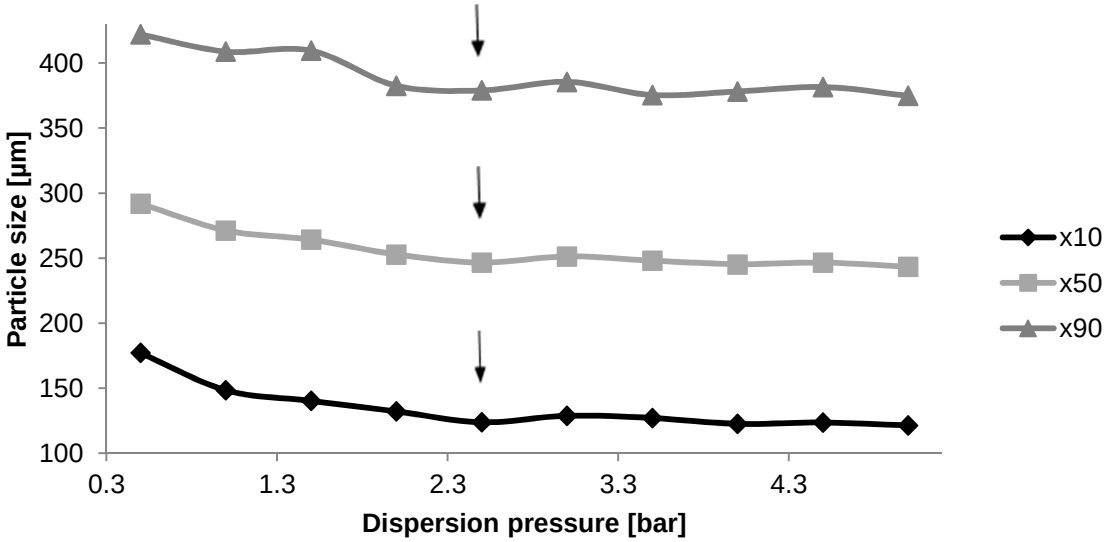

Figure 2: Influence of the dispersion pressure on the particle size distribution. x10 x 50 x90. The arrows indicate where the minimum in particle size is reached.

It can be clearly observed that, the higher the dispersion pressure, the smaller are the values of x10, x50 and x90. When a pressure of 2.5 bar is reached, a minimum in particle size is observed and afterwards the particle size reaches a plateau. Therefore, dispersion pressures of 0.5 bar and 2.5 bar were chosen and the results are presented below. In Figure 3 the normalized Q3 distribution of the results of the dispersion pressure of 0.5 bar is shown.

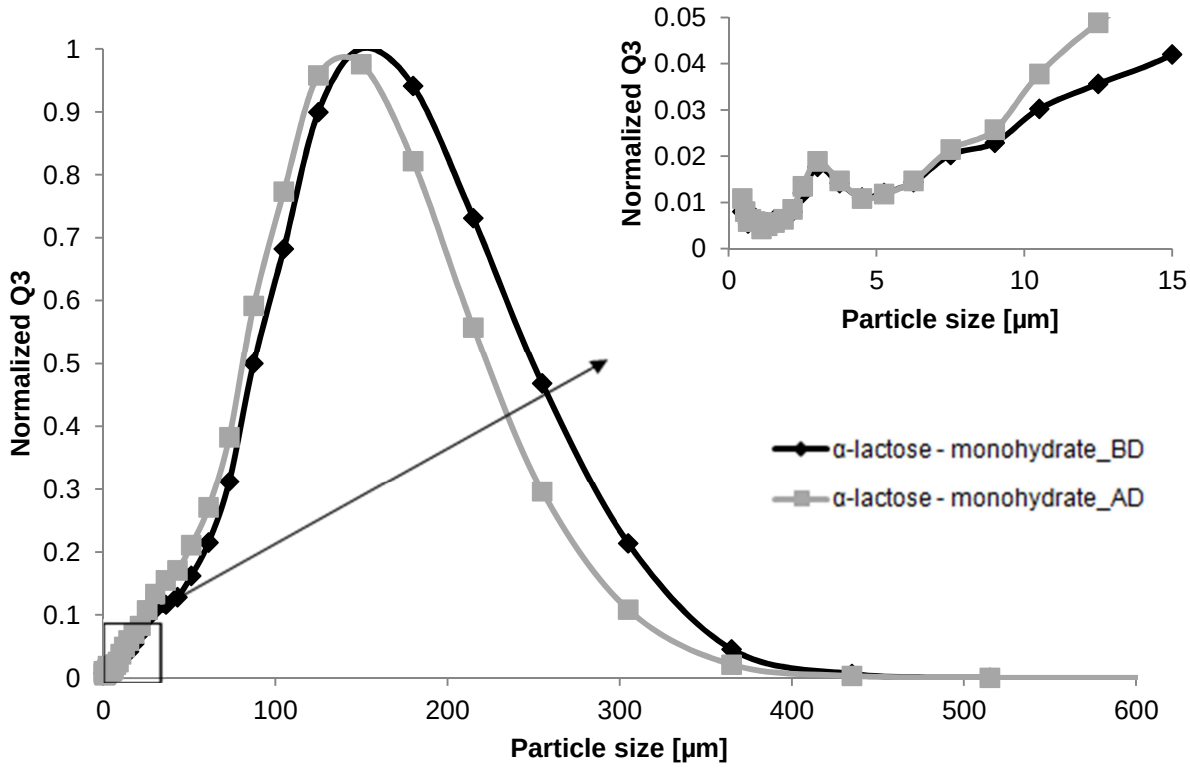

Figure 3: Normalized Q3 distribution – HELOS (0.5 bar dispersion pressure) BD – Before decantation AD – After decantation

From the Q3 curve of the 0.5 bar investigation it can be observed that the span of the particle size distribution is decreasing after decantation. Again the particle size is decreasing after processing the inhalation carrier (Table 2). No significant changes in the fine particle fraction (here defined as particles: < 15µm) can be observed. The Q2 and Q0 distribution can be found in Appendix 2. In Figure 4 the Q3 distribution curves of the measurements using a dispersion pressure of 2.5 bar are depicted.

Table 2: Particle size before and after decantation (±sd) – Helos (0.5bar dispersion pressure)

	x10 [µm]	x50[µm]	x90[µm]	Span of particle size
Before decantation	177.0±0.30	291.8±1.58	422.1±3.71	0.84
After decantation	148.4±0.70	271.3±2.04	408.8±4.03	0.96

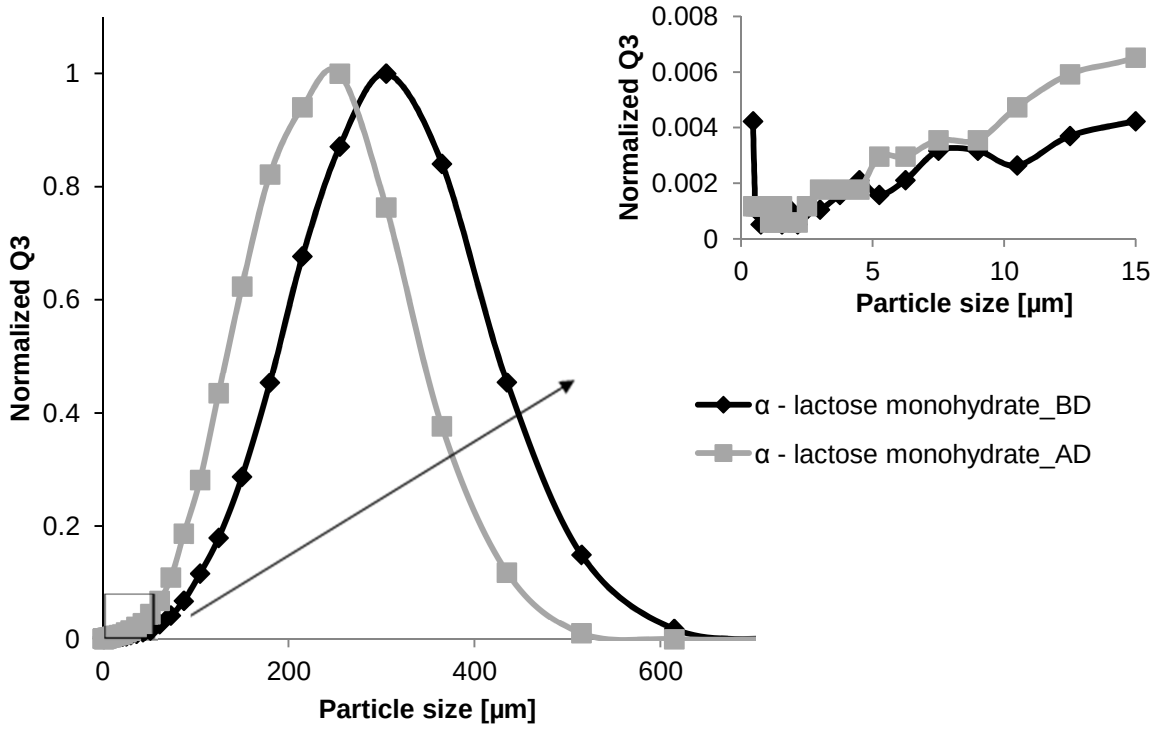

Figure 4: Normalized Q3 distribution – HELOS (2.5 bar dispersion pressure); BD – Before decantation AD – After decantation

When using a higher pressure the difference of the particle size between before and after decantation is more significant. Again particle size is decreasing and the span of the particle size distribution is increasing (Table 3). The amount of particles < 15µm cannot be identified very well. The Q0 and Q2 data (data in Appendix 6.1) of the measurements was analyzed as well, but again the differences before and after decantation were found to be not significant and difficult to interpret.

Table 3: Particle size before and after decantation (±sd) – Helos dry dispersion (2.5 bar dispersion pressure)

	x10[µm]	x50[µm]	x90[µm]	Span of particle size
Before decantation	124.57 ± 0.56	246.81 ± 0.52	379.33 ± 1.49	1.03
After decantation	107.75 ± 0.84	225.5 ± 0.92	358.12 ± 3.45	1.11

Therefore, the particle size distribution was also investigated using the Mastersizer 2000. With the latter, only a pressure of 0.5 bar can be used to disperse the powder. Once more the Q3 distribution was analyzed and it was noticeable that the particle size, as well as the span of the particle size, is decreasing after decantation (Figure 5, Table 4).

Table 4: Particle size before and after decantation (±sd) – Mastersizer (0.5 bar dispersion pressure)

	x10[µm]	x50[µm]	x90[µm]	Span of particle size
Before decantation	123.9±3.05	237.9±2.41	626.3±110.6	2.10
After decantation	83.33±11.9	181.0±12.5	340.0±44.52	1.42

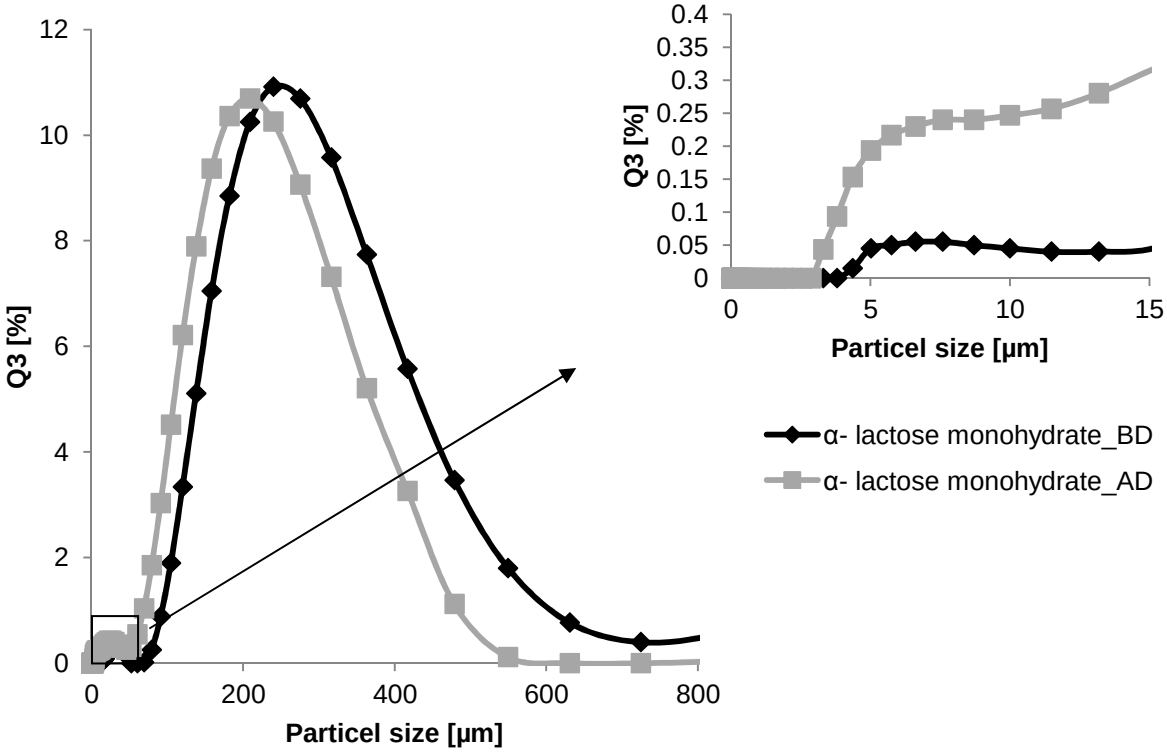

Figure 5: Q3 distribution – Mastersizer (0.5 bar dispersion pressure) BD – Before decantation AD – After decantation

Moreover the Q3 distribution of the particle size fraction < 40µm is increasing. Again the Q0 distribution was analyzed (data shown in Appendix 6.2). One of the explanation for the results obtained from the data analysis of the investigated dry particles, can be described with the following scenario (Figure 6): fine carrier particles stick on the surface of the larger lactose particles before the decantation process.

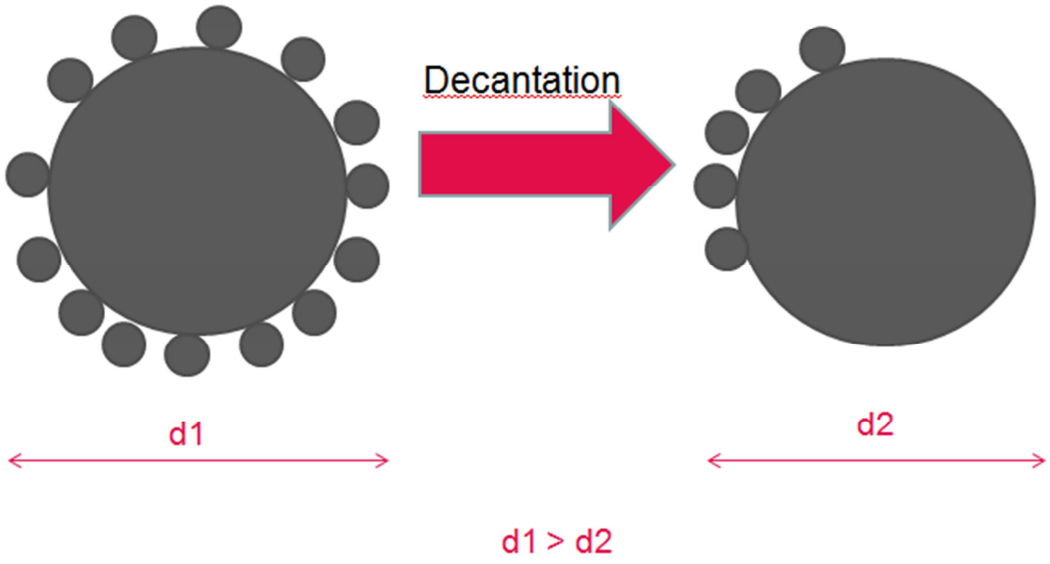

Figure 6: Assumption about particle size measurement

Although a dispersion pressure of 2.5 bar was used, it was not possible to de-agglomerate all the fine particles stuck on the surface of the larger ones before the decantation process. After decantation the majority of the fine particles was removed because of the process and, therefore, the particles seem to be smaller when investigating the particle size. Furthermore, after decantation the binding energies between the particles are decreasing according to the processing with absolute ethanol. Thus, the remaining fine particles can be removed more easily and in a higher amount than before the processing, when using a higher dispersion pressure. These assumptions may explain why the particles seem to be smaller after the decantation process then before, although these phenomena can lead to a bias of the results. In fact, another explanation for the smaller particle size observed after decantation is the dissolution of the carrier surface due to the water content within the ethanol (according to the hygroscopicity of absolute ethanol) used for the decantation, which could have induced a slightly decrease in the size of the particles, since the shift of x_{10}-x_{90} to smaller particle sizes was obtained with all measurements.

To investigate the source of this problem the particle size distribution was also measured using the wet decantation cell of the Mastersizer, implementing 20 sec of ultrasound before each measurement, in order to allow disaggregation of the fines from the carrier surface (Figure 7).

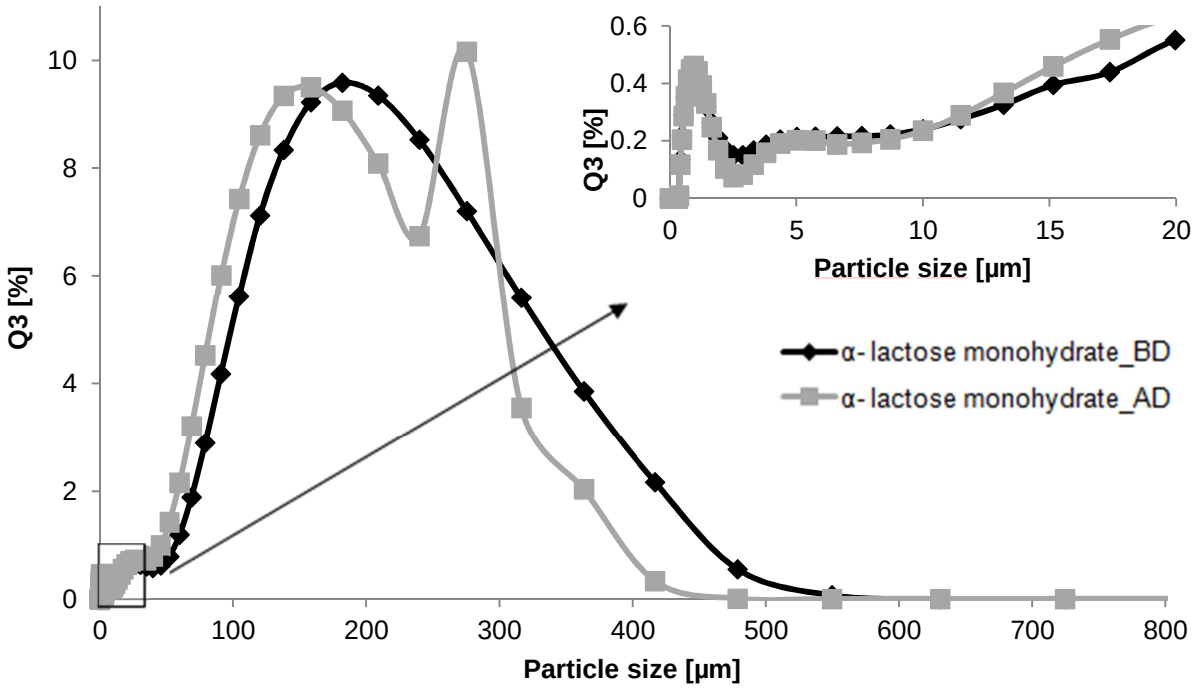

Figure 7: Mastersizer wet dispersion – applying 20sec ultrasound before the measurement BD – Before decantation AD – After decantation

In Figure 7 no significant differences in the particle size before and after decantation can be observed. Although the region of particle < 5 µm seems to have a better resolution than in dry dispersion, no differences in small particle size part between the treated and starting material can be observed in this particular region of the particle size distribution. In Table 5 the particle size of the unprocessed and processed lactose carrier is depicted. Again, the particle size is decreasing after decantation and the span of the particle size distribution is increasing slightly.

Table 5: Particle size before and after decantation (±sd) – Mastersizer

	x10[µm]	x50[µm]	x90[µm]	Span of particle size
Before decantation	34.99±17.9	152.1±17.72	267,0±18.10	1.66
After decantation	29.62±6.03	127.5±5.23	246.1±10.5	1.69

Next, the particle size distribution of the lactose carrier dispersed in ethanol absolute was measured with the HELOS. Before performing the measurement 20 seconds ultrasounds were applied to each sample (Figure 8).

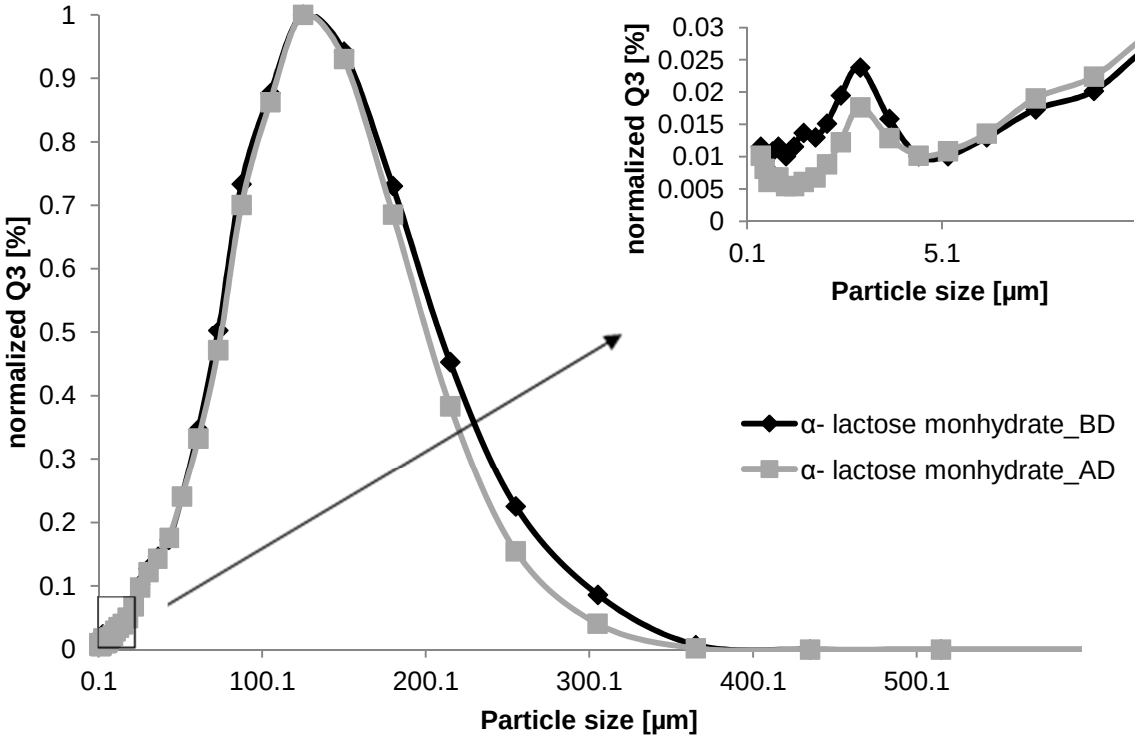

Figure 8: Normalized Q3 distribution using wet dispersion Helos (applying 20 sec ultrasound before the measurement) BD – Before decantation AD – After decantation

It can be observed that the particle size is not changing significantly after decantation and the span of the particle size distribution is decreasing (Table 6). Furthermore the fine particle fraction is decreasing after processing of the lactose carrier.

Table 6: Particle size before and after decantation (±sd) – Helos wet dispersion - appyling 20sec. ultrasound before the measurement

	x10[µm]	x50[µm]	x90[µm]	Span of particle size
Before decantation	35.43±0.45	121.4±1.12	219.5±1.92	1.52
After decantation	37.10±0.42	120.4±0.49	210.0 ±1.66	1.43

To summarize the data presented herein:

- different techniques, namely dynamic image analysis and laser diffraction (2 different equipments) were used in this study
- different dispersion methods, dry (using different pressures) and wet (applying 20 sec ultrasound before the measurement), were used to investigate the particle size distribution of the lactose carrier

After the decantation, an overall decrease in particle size was observed within all used methods. Furthermore the span of the particle size was found to be increased. The principle of dynamic light scattering was found not to be sensitive enough for the characterization of the decanted samples, due to the wide size differences between the carrier and the adhering fines. When using the laser diffraction technique with the dry dispersion unit, the measurement was found to be sensitive to the dispersion pressure used,as various pressures were investigated to find the ideal settings for the particle size measurement of the lactose carrier. After having found the optimum pressure, it was observed that the resolution in the fine particle fraction region (here: < 15µm) was not high enough to determine differences in the generated Q3 distributions before and after decantation. Thus, the measurements where conducted in the wet dispersion cell, applying 20 seconds ultrasound before each measurement

By comparing the wet dispersion cell results, it was observed, that no significant changes in the particle size before and after decantation occured when using the Helos equipment. Furthermore, the span of the particle size of the lactose carrier was found to decrease when using this technique. By setting the focus on the particle size region < 15µm it was possible to observe that the volume distribution was decreasing after the decantation process. This effect was expected at the very beginning of this study.

Therefore, it can be assumed that the wet dispersion method with 20 sec ultrasound (Helos) seems to be the best method to determine the removal of the fine particle fraction after decantation. Thus, this method was used for all further particle size measurements presented in this Thesis.

3.2 Preparation of a 1kg batch

To remove the adherent fines of the lactose carrier, 1 kg of the non sieved fraction of the carrier powder was used and processed by wet decantation. After drying of the treated lactose, several powder properties were investigated to compare the physico-chemical attributes of the lactose before and after processing. Additionally, a stability study was performed on the product according to ICH guidelines (35).

Determination of the water content

The water content of the powders was determined by Karl Fischer titration (Figure 9). The results show no significant change in the water content before and after decantation and after the stability study.

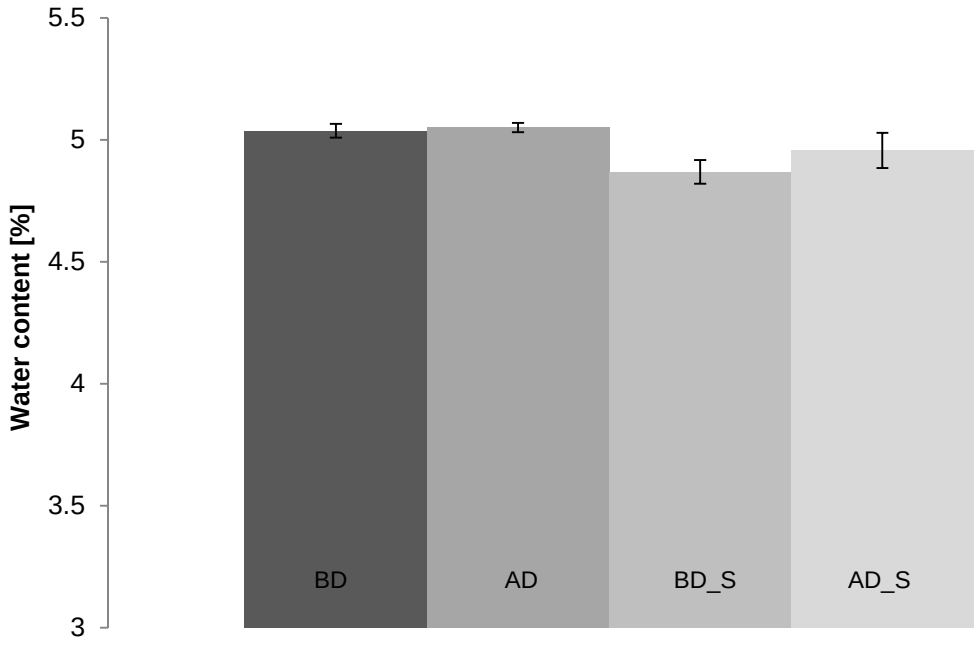

Figure 9: Water content of the powders before decantation (BD), after decantation (AD) and before decantation exposed to stability study (BD_S) and after decantation exposed to stability study (AD_S).

Particle size and shape characterisation

The particle size of the carrier was investigated by wet dispersion using ethanol absolute as fluid and applying ultrasound for 20 second before each measurement (Figure 10) (for detailed information regarding the experimental set up, see: Chapter 1).

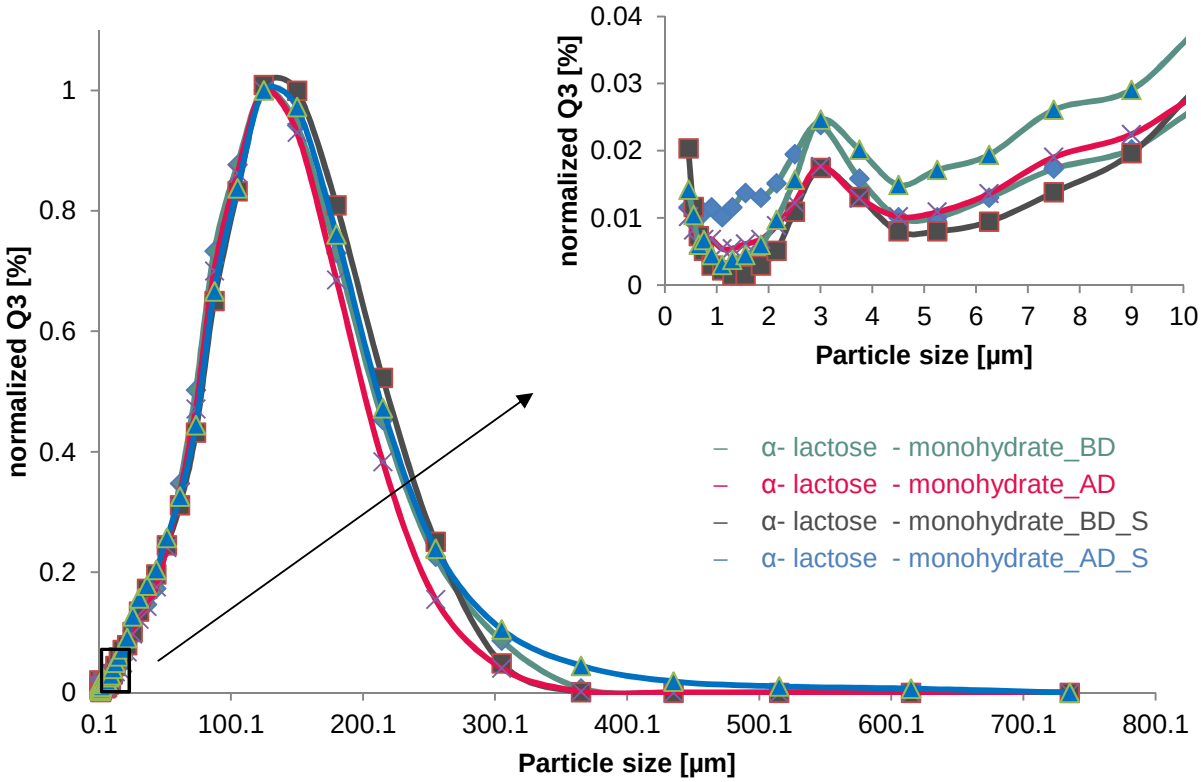

Figure 10: Particle size distribution of the lactose carrier before decantation (BD), after decantation (AD) and before decantation exposed to stability study (BD_S) and after decantation (AD_S).

In Figure 2 it can be observed that after decantation the fine particles fraction present on the carrier was removed. Additionally to the investigation of the particle size distribution, the shape of the lactose carrier particles was investigated. The shape of the particle is important for the dry powder inhaler performance as it determines the behaviour of the particle in the airstream. Furthermore, it defines the contact area and the adhesion forces between the particles (42). The particle shape was measured by dynamic image analysis. Herein, we present data for aspect ratio, convexity and sphericity (Figure 11,12 and 13).

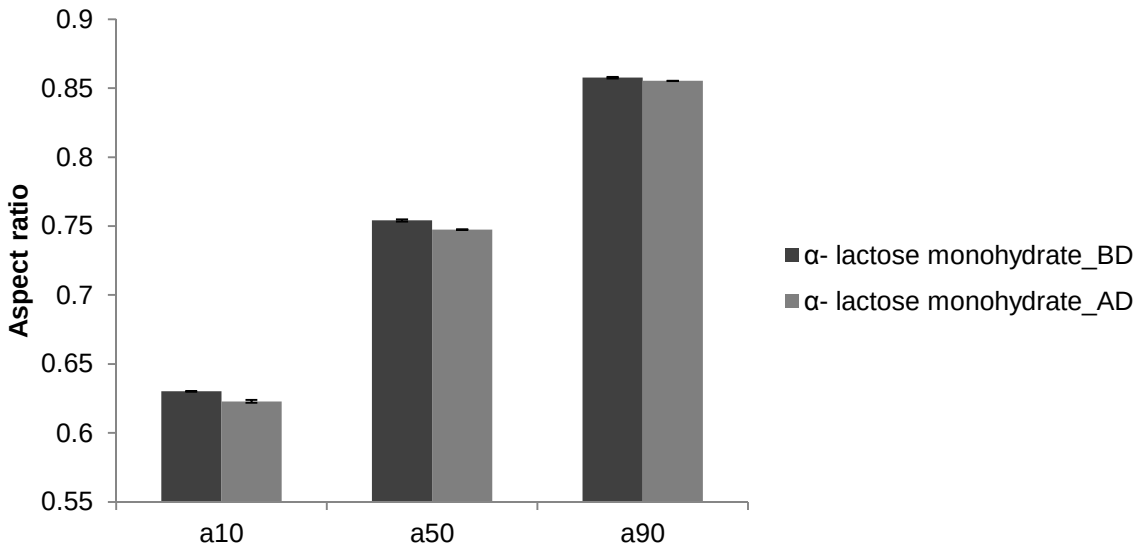

Figure 11: Aspect Ratio of the lactose before (BD) and after decantation (AD). a10 is the 10th percentile of the aspect ratio distribution, a50 is the 50th percentile of the aspect ratio distribution, a90 is the 90th percentile of the aspect ratio distribution.

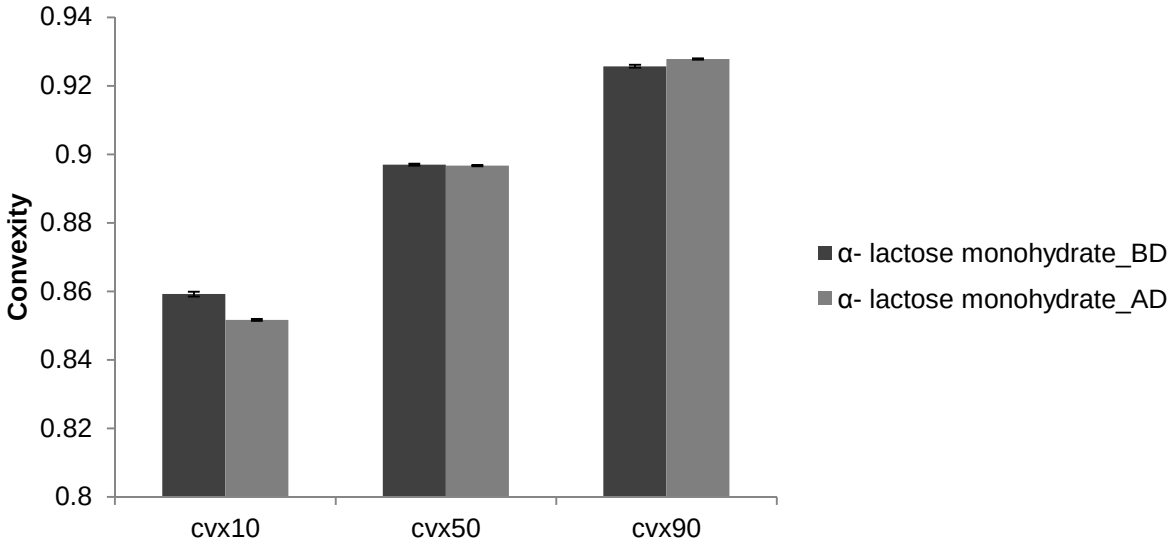

Figure 12: Convexity of the lactose carrier before (BD) and after decantation (AD). cvx10 is the 10th percentile of the convexity distribution, cvx50 is the 50th percentile of the convexity distribution, cvx90 is the 90th percentile of the convexity distribution.

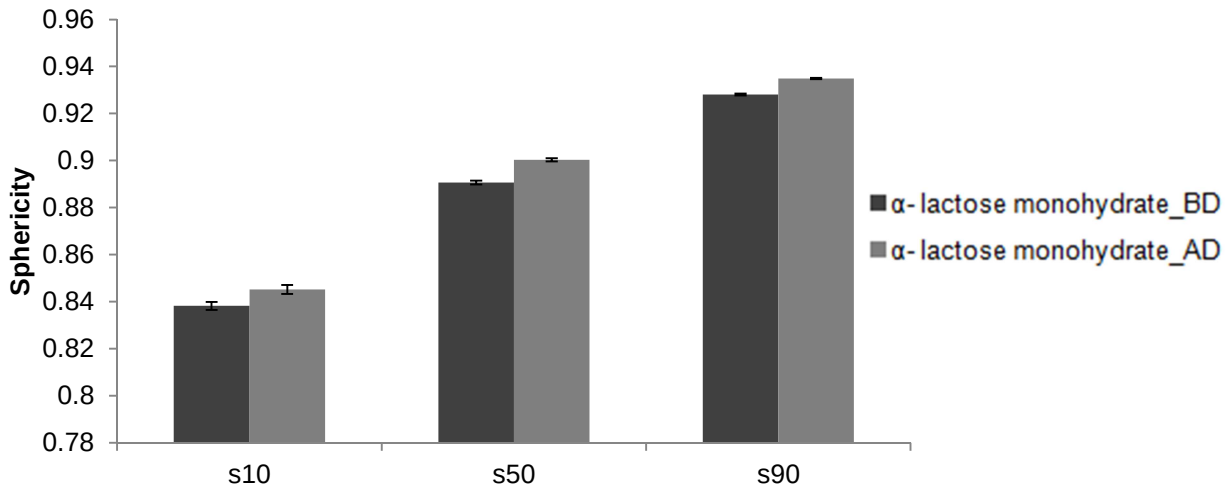

Figure 13: Sphericity of the samples before (BD) and after decantation (AD). s10 is the 10th percentile of the sphericity distribution, s50 is the 50th percentile of the sphericity distribution, s90 is the 90th percentile of the sphericity distribution.

The aspect ratio was slightly decreasing after decantation, while sphericity and convexity were found to increase. The decrease of cv10 indicates that smaller particles are more concave shaped. Moreover, it can be assumed that particles became more spherical and similar in shape.

Scanning electron spectroscopy and determination of roughness

To confirm the removal of fines from the carrier surface, scanning electron microscopy pictures were acquired (Figure 14).

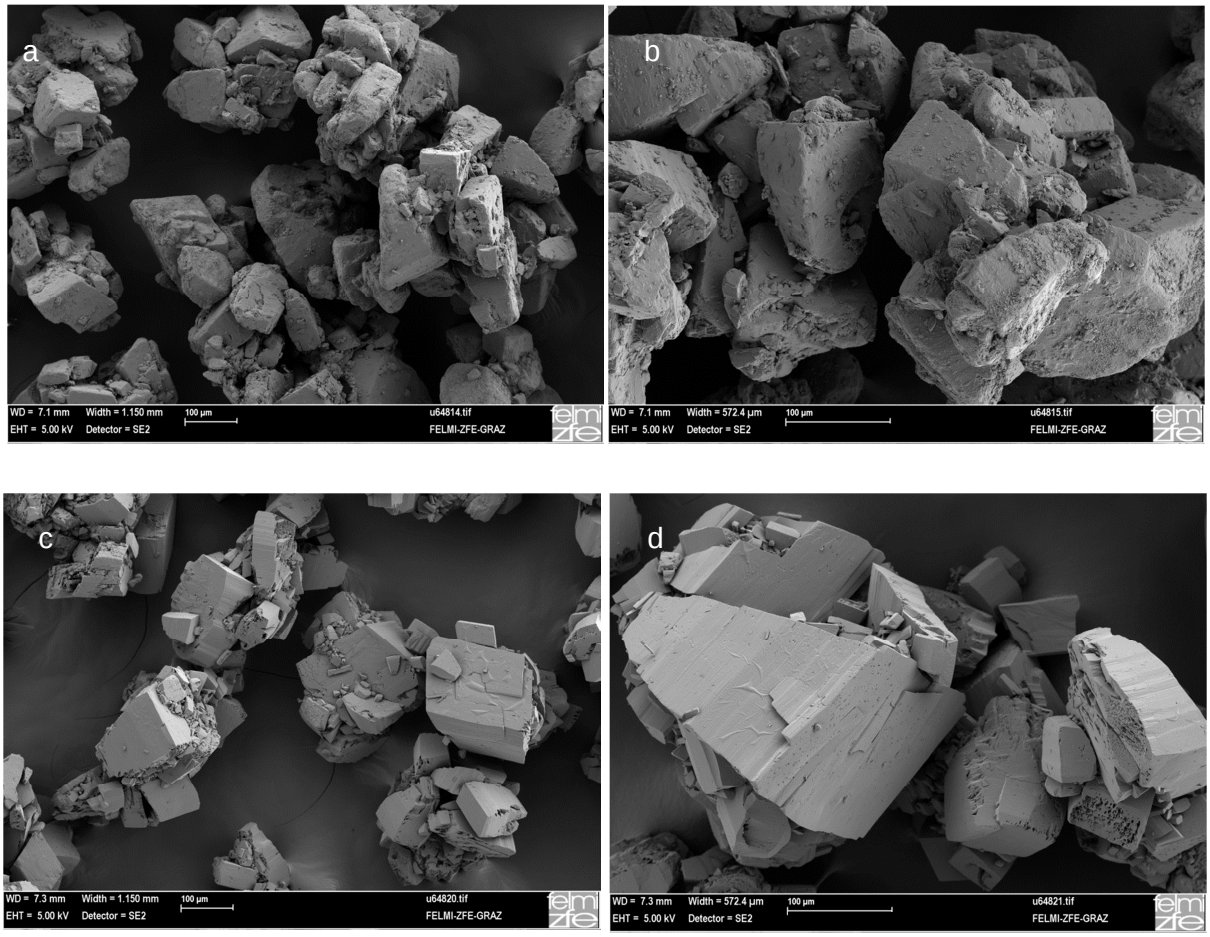

Figure 14: Scanning electron microscopy pictures of α- lactose monohydrate before (a,b) and after decantation (c,d).

It was clearly observed that the adherent fines were removed and that the surface remained unchanged even after the stability study (Figure 15). Interestingly, it can be observed that the material became more porous after decantation.

According to the SEM pictures was clearly observable that the surface of the lactose appeared smoother after decantation and that the majority of fine particles were removed. During the storage at elevated conditions the product appearance did not change.

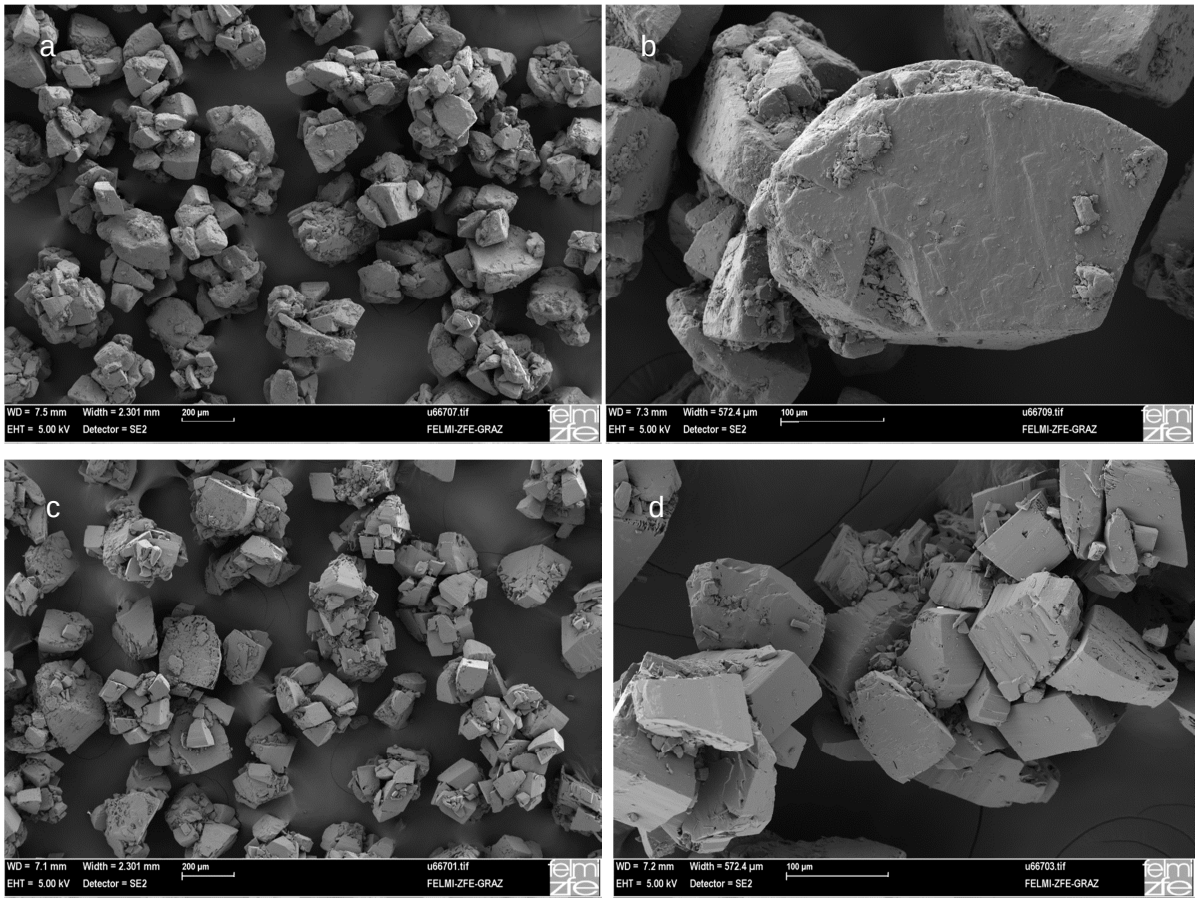

Figure 15: SEM pictures of the carrier material after stability study before decantation (a,b) and after decantation (c,d).

From the SEM pictures it was possible to calculate the surface roughness of the samples. To do so about 15 – 30 section areas with a size of 28.5 x 28.5 µm, taken from the samples surfaces, were investigated. This was done for the lactose carrier before and after decantation as well as after stability study (Figure 16 and17). From Figure 17 it can be observed that the roughness, which is expressed by the root mean square deviation (Rq) [µm], differs statistically significant.

According to the presented data, the samples after decantation were smoother as fines are removed.

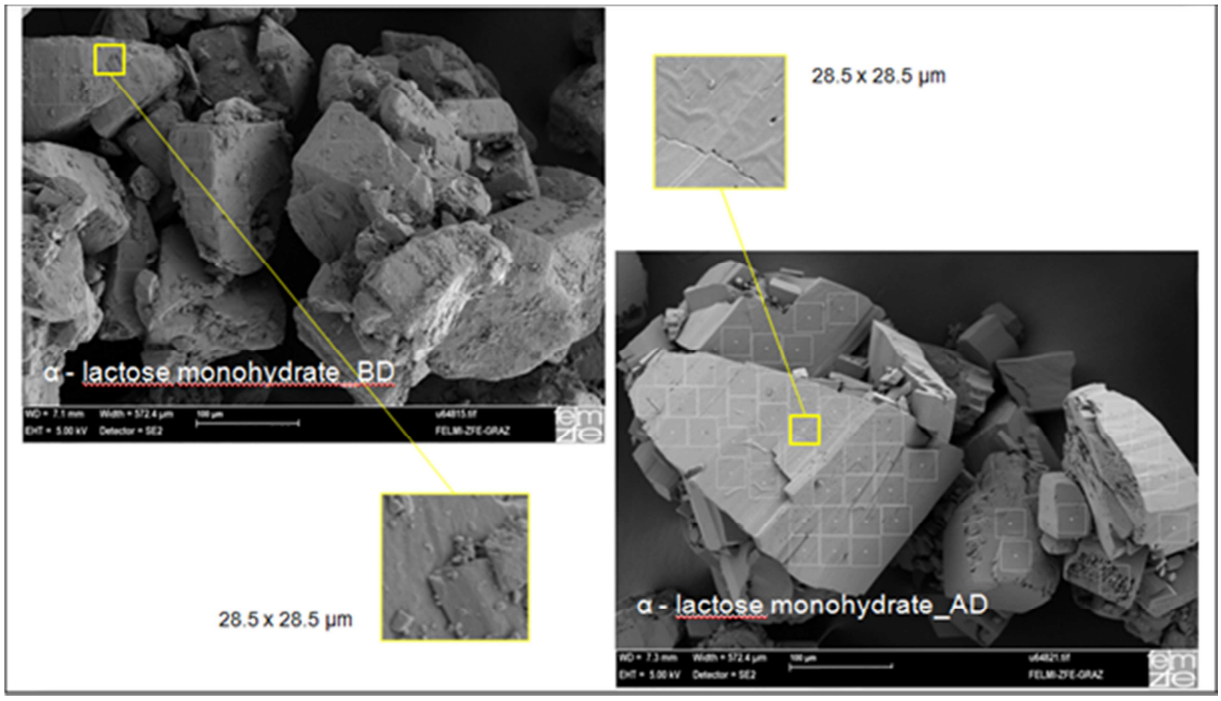

Figure 16: Surface Roughness determination of the lactose carrier before and after decantation

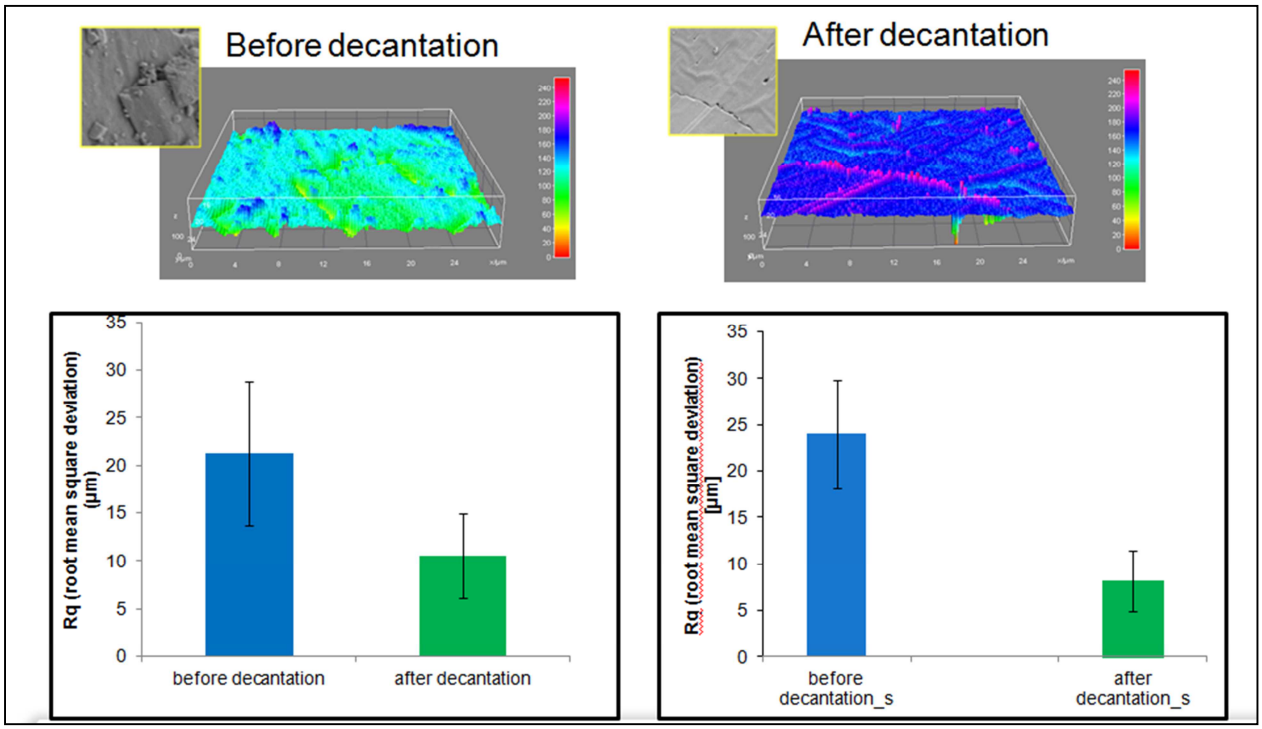

Figure 17: Surface roughness of α – lactose monohydrate before and after decantation and after stability study (_s).

Solid state characterization

To analyze the crystallinity state of the samples, differential scanning calorimetry (DSC) (Figure 18) and wide angle X–ray scattering (WAXS) measurements were performed (Figure 19).

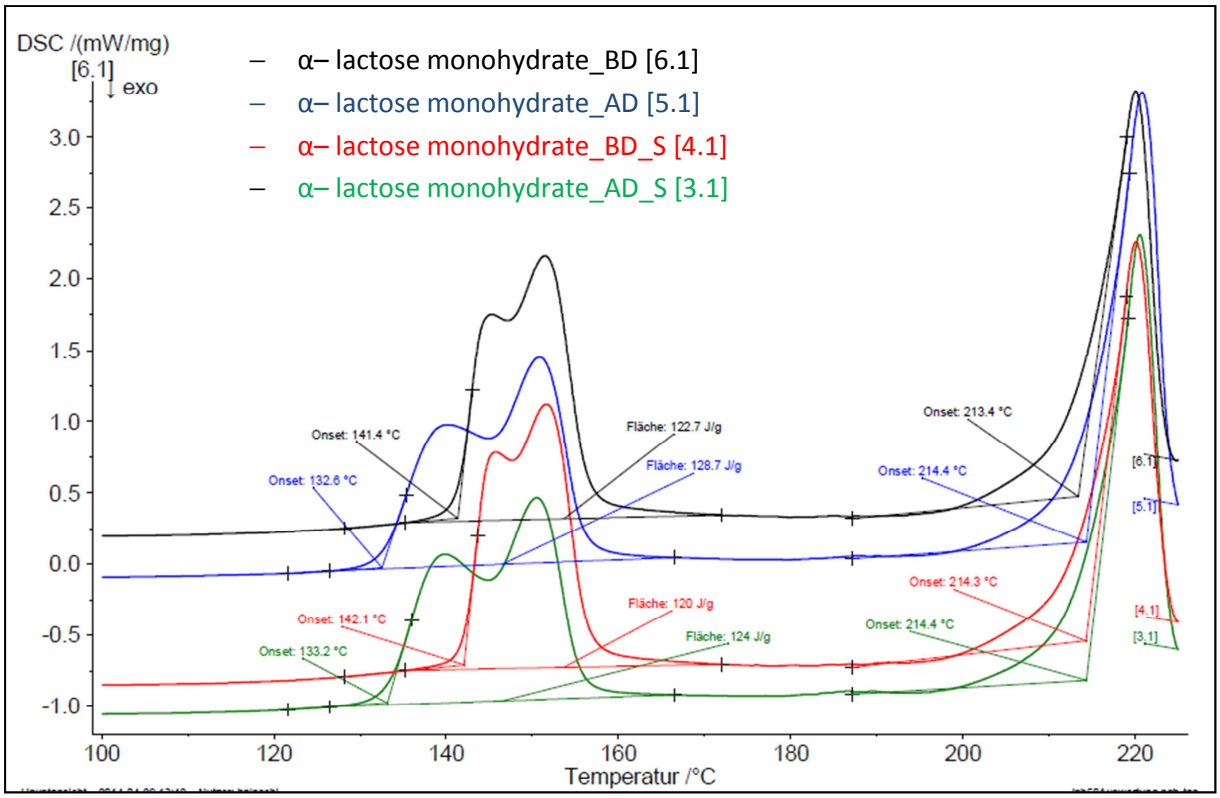

Figure 18: Differential scanning calorimetry (DSC) graphs before (BD) and after (AD) decantation and before decantation exposed to stability study (BD_S) and after decantation (AD_S).

The peaks observed in Figure 18, were identified according to the literature (43), as follow:

- 144°C: dehydration of crystalline water of α- lactose monohydrate (endothermic peak)
- ~ 170°C: crystallization of unstable anhydrous α-lactose into crystalline ß/α compound (ß/α = ~1:1)
- ~210-220°C: melting of α- lactose monohydrate (endothermic peak)

It appears that the samples under investigation were all a mixture of α–lactose monohydrate and β–lactose, but the curves before and after decantation had more proportion wise α–monohydrate. The peaks from 130–155°C indicated the dehydration event. After decantation the peak around 150°C was slightly broader than before decantation. This was likely due to a higher amount of anhydrous α-lactose. However, after stability study the DSC thermograms looked similar, and consequently, their solid state did not change during accelerated storage conditions.

Additionally WAXS spectra were recorded to investigate the crystallinity of the samples (Figure 19).

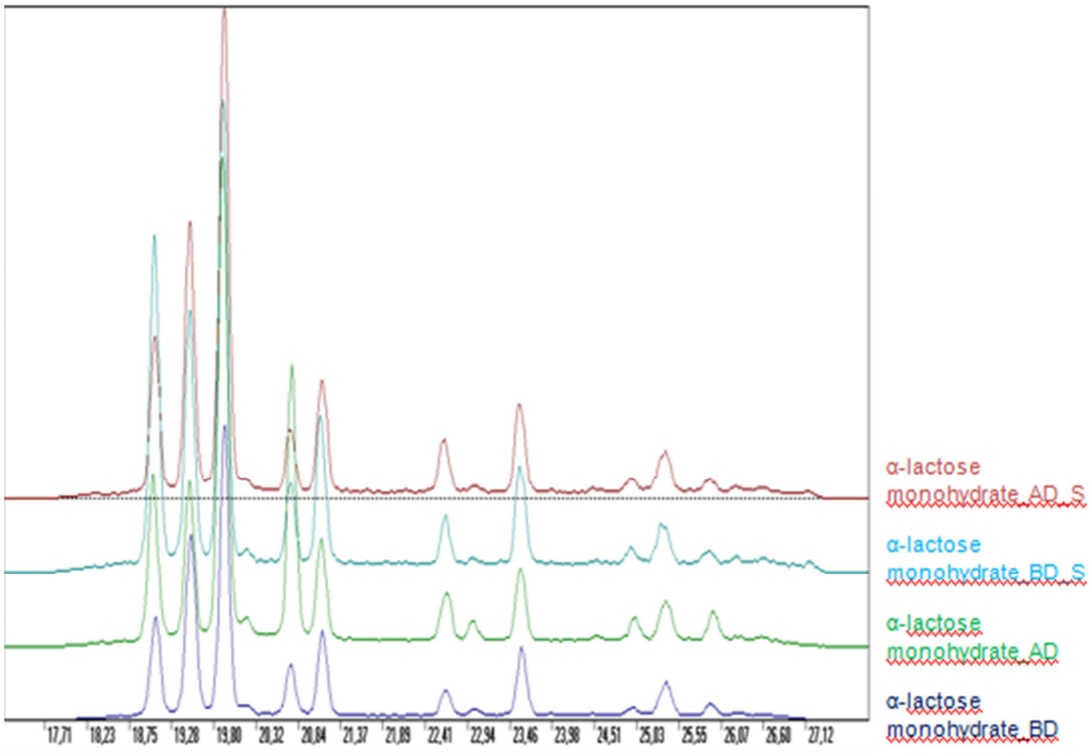

Figure 19: WAXS spectra of before (BD) and after decantation (AD) and before decantation exposed to stability study (BD_S) and after decantation (AD_S).

The samples look similar before and after decantation as well as after stability study. Therefore it can be assumed that the crystallinity did not change as a consequence of the wet decantation process.

When using small angle scattering (SAXS) it is possible to determine the inner surface of the powders (Figure 20), which is expressed by the parameter k2/Q. In Figure 20 it can be observed that the parameter k2/Q is not changing as a consequence of the decantation process as well as after the stability studies.

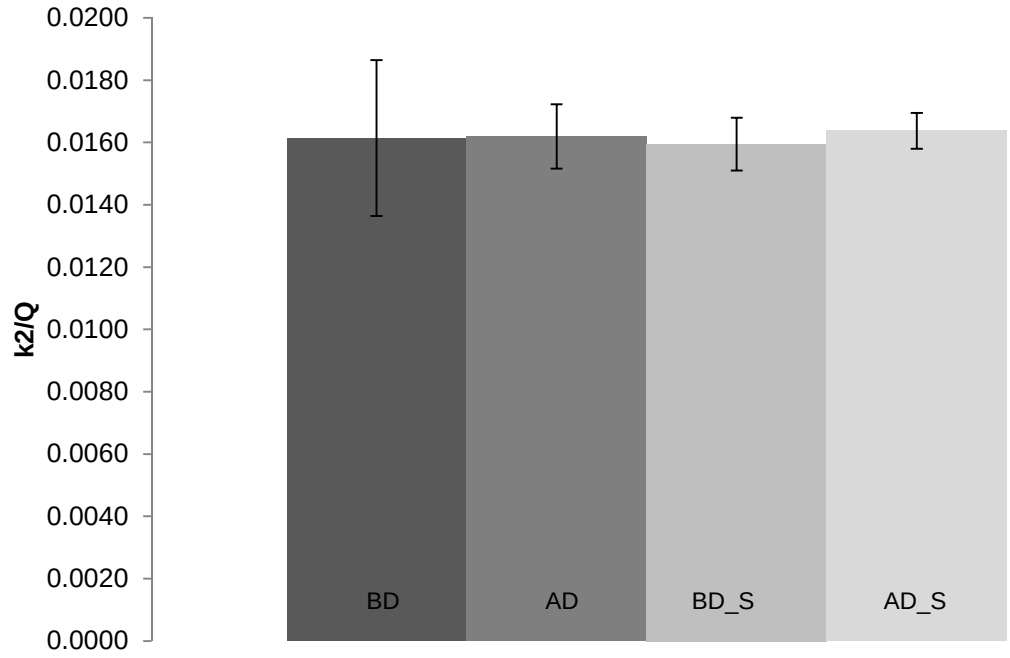

Figure 20: SAXS results of the lactose carrier before (BD) and after decantation (AD) and before decantation exposed to stability study (BD_S) and after decantation (AD_S).

Characterization of flowability

It was expected that the elimination of the particle surface asperities was going to provide an improvement of the powder packing and flow properties, according to the reduction of the friction between particles (increasing sphericity of the particles after decantation) and to more dense packing of the powder bed (44). In fact, the higher amount of fines are present within the powder, the poorer is the flowability (45). Therefore, the lactose carrier samples before and after decantation were analyzed according to their flowability. The flowability of the samples undergoing the stability study was not performed. The following parameters were determined: the basic flow energy (BFE), the angle of internal friction, the flow function (ff_c) as well as the angle of repose and the average friction coefficient.

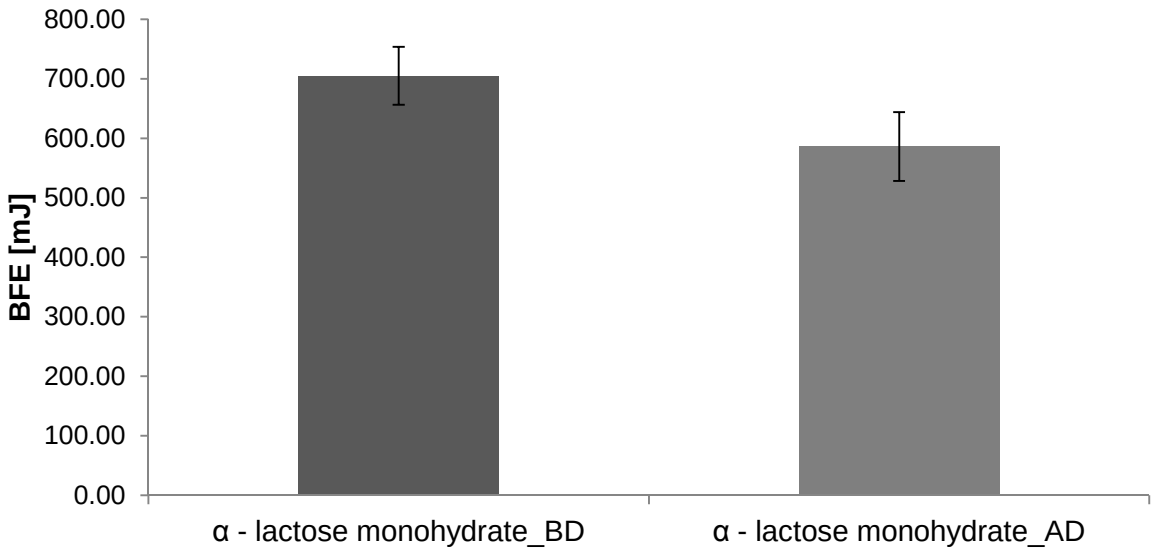

Figure 21: Basic flow energy (BFE) of the lactose carrier before (BD) and after decantation (AD).

From (Figure 21) it can be seen that the basic flow energy is decreasing after decantation. This means that after decantation less energy is needed to start the powder flow, which indicates improved powder flowability. For non-cohesive powders particularly, the basic flow energy is relatively high. Flow properties such as flow function and angle of internal friction were also obtained (Table 7). The flow function (ffc) of a powder is the ratio of consolidation stress σ1 and unconfined yield stress σc. The larger ffc is (e.g. the smaller the ratio of unconfined yield strength to the consolidation stress) the better the bulk flows (Table 8). The angle of repose (AIF) is derived from the angle of the best-fit-line to the x-axis from the Mohr circle.

Table 7: Flow function (ff_c) and angle of internal friction and their standard deviation (± sd)

	ff_c (± sd)	**Angle of internal friction (± sd)**
Before decantation	9.03 (± 1.05)	32.81 (± 1.16)
After decantation	8.81 (± 1.47)	34.86 (± 4.06)

Table 8: Classification of the powder flowability by flow index (46)

Flowability	Hardened	Very cohesive	Cohesive	Easy flowing	Free flowing
Flow index (ff_c)	< 1	< 2	< 4	< 10	>10

The angle of repose was also determined (Table 9); It is defined as the steepest angle of descent or of the slope relative to the horizontal plane when a material on the slope face is on the verge of sliding. This angle ranges between 0° and 90°. Additionally the average friction coefficient was investigated (Table 9).

Table 9: Average friction coefficient and angle of repose

	Average friction coefficient	Angle of repose [°]
Before decantation	0.56	29.25
After decantation	0.57	29.53

From Table 9 it can be observed that the angle of repose was not changing before and after decantation. Moreover the average friction angle was constant. Additionally the bulk and tapped density were investigated. From these density values the Carr index (CI) and the Hausner ratio (HR) can be calculated (Table 10).
The Carr index indicates the compressibility of a powder.

Table 10: Tapped and bulk density, Hausner ratio (HR), Carr index (CI)

	ρ (bulk) [g/mL]	ρ (tapped) [g/mL]	Hausner ratio (HR)	Carr index (CI)
Before decantation	0.58 ± 0.03	0.69 ± 0.02	1.17± 0.01	14.86 ± 0.9
After decantation	0.61 ± 0.002	0.78 ± 0.005	1.28 ± 0.007	22.0 ± 0.5

When comparing the data, the Hausner ratio is increasing after decantation. According to Table 11 the flow character is therefore decreasing from good to passable. The same behaviour can be obtained for the Carr index.

Table 11: Flowability values (47)

Carr index (CI)	Hausner Ratio (HR)	Angle of repose [°]	Flow character
<10	1.00 – 1.11	25 – 30	Excellent
11 – 15	1.12 – 1.18	31 – 35	Good
16 – 20	1.19 – 1.25	36 – 40	Fair
21 – 25	1.26 – 1.34	41 – 45	Passable
26 – 31	1.35 – 1.45	46 – 55	Poor
32 – 37	1.46 – 0.59	56 – 65	Very poor
>38	> 0.60	>66	Very, very poor

The CI values indicate that the smoothing of the particles, due to the decantation process, hinders the packing and that the flowability is worse after decantation. This outcome is opposite to the data obtained using the basic flow energy results and it can be explained by the different methodology used. In fact, some of them are operator depending and some of them not, therefore the comparison between the two methods can be challenging. However, the CI values seem to be more reliable as the BFE is dependent from a lot of particle attributes (e.g water content, particle shape, particle surface texture).

Infrared Spectroscopy

To prove the complete removal of ethanol from the decanted material, ATR–FT–IR measurements were performed (Figure 22).

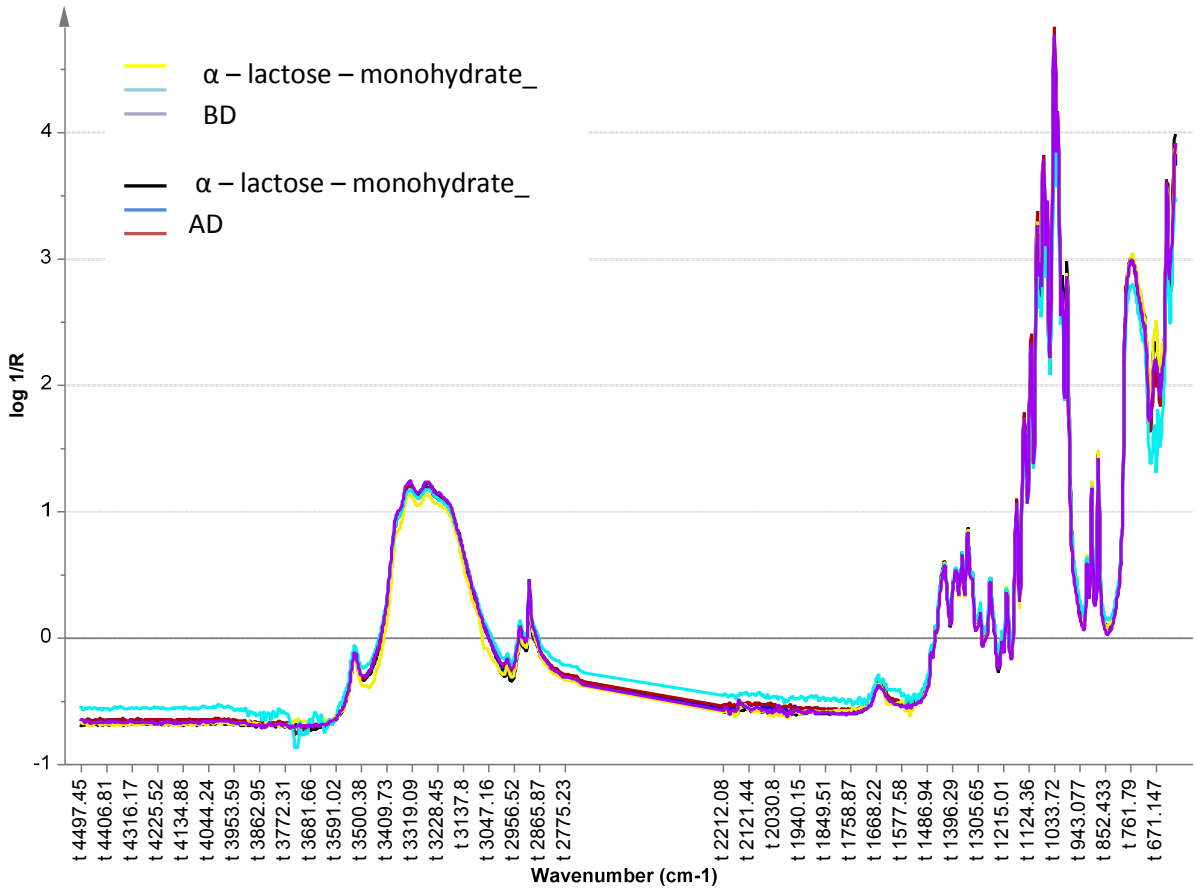

Figure 22: SNV corrected ATR-FT–IR spectra of the lactose carrier before (BD) and after (AD) decantation.

In Figure 22 it can be observed that no differences before and after decantation are occurring. This indicated that the used ethanol was completely removed. Ethanol has a characteristic IR absorption in the area of 3500 – 3200 cm^{-1} (O - H stretching) as well as in the area of 1260 –1050 cm^{-1} (C – O stretching) (Figure 23), which are clearly absent in the decanted samples.

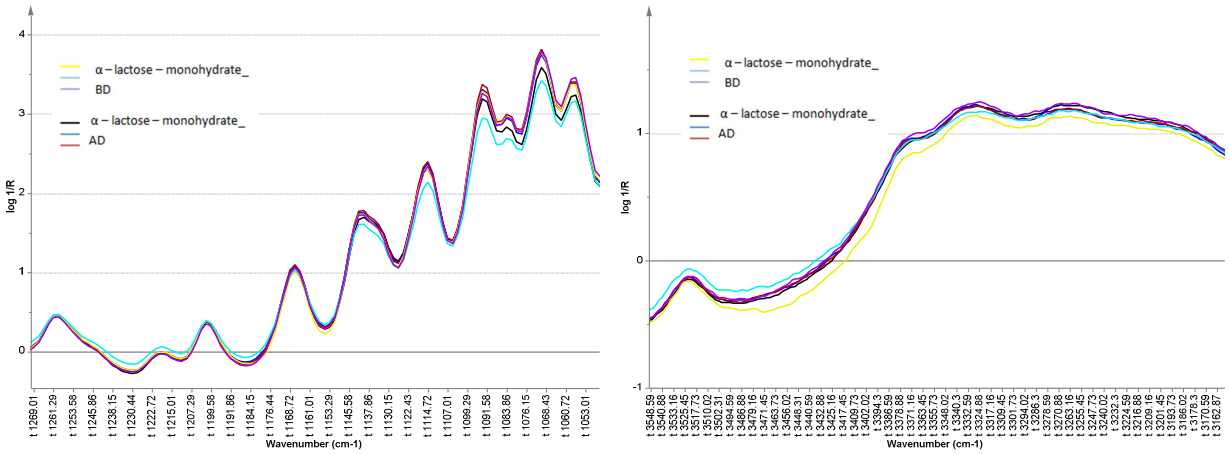

Figure 23: Ethanol stretching IR absorption areas

To summarize the data presented in this paragraph, the lactose carrier was characterized before and after decantation, to prove the success of the surface modification process. According to the particle size measurements, SEM pictures and roughness measurements, the desired outcome of the decantation was achieved. Additionally, slight differences in powder attributes of the material before and after decantation were obtained, as observed by the DSC and flowability measurements. No differences between the unprocessed and processed lactose were observed via WAXS and ATR–FT–IR. After one month stability study under accelerated storage conditions of 40 ± 2 ºC/ 75 ± 5 % RH no major changes were observed, indicating that the decanted lactose successfully sustained accelerated stress condition, and stability up to 3 months can be insured.

3.3 Design of experiment (DoE) for the decantation process

The aim of the study was to improve the understanding of the wet decantation process by studying the influence of various factors on the decantation technique. Therefore, 50g of the lactose carrier were decanted , varying the following factors: the solvent/solid ratio, the mixing time and the number of cycles. The sedimentation time of 1 minute was set as a constant factor. A 3^2 design of experiments (DoE) with a center point run in triplicate was performed, as shown in Table 12.

Table 12: Worksheet DOE

Run order	Factor list		
	Solvent/solid ratio	**Mixing time**	**n°cycles**
N1	2	2	5
N2	3	2	5
N3	2	20	5
N4	3	20	5
N5	2	2	15
N6	3	2	15
N7	2	20	15
N8	3	20	15
N9	2.5	11	10
N10	2.5	11	10
N11	2.5	11	10

After performing the 11 experiments, the samples were dried under the fume hood for 3–4 days and then stored in desiccators on silica. Subsequently, the particle size was determined

as well as the BET surface area. To prove if the process was successful, SEM pictures were taken from the decanted material, as well as from the starting material, and the roughness of the surface was calculated using the software Image J. The aforementioned parameters were used as response factors for the DoE (Table 13).

Table 13: Response List for DoE

Run order	Response factors		
	x_{10} [µm]	Roughness [µm]	BET [m^2/g]
N1	34.95	16.77	0.25
N2	45.17	13.76	0.22
N3	40.11	16.28	0.12
N4	37.64	17.54	0.19
N5	41.53	13.46	0.14
N6	37.55	11.62	0.15
N7	45.50	13.35	0.25
N8	50.20	7.44	0.15
N9	43.75	15.49	0.14
N10	59.39	11.40	0.12
N11	54.18	15.97	0.15

The model was fitted with a PLS (partial least square) regression. PLS is not based on the assumption of independent and precise X–variables. Thus, PLS is a class of methods for modeling relations between sets of observed variables, by means of latent variables (48). The PLS model parameters arising from this latent variable projection e.g., scores and weights (loadings), may be used for model interpretation. This latent variable model may also be transferred into a set of PLS regression coefficients, which may be easier to interpret than PLS weights in a given application (49). At the beginning of the analysis all factors and interactions were included to assess the significance of the factors as well as the interactions.

The following summary of fit was created with the already cited parameters (Figure 24).

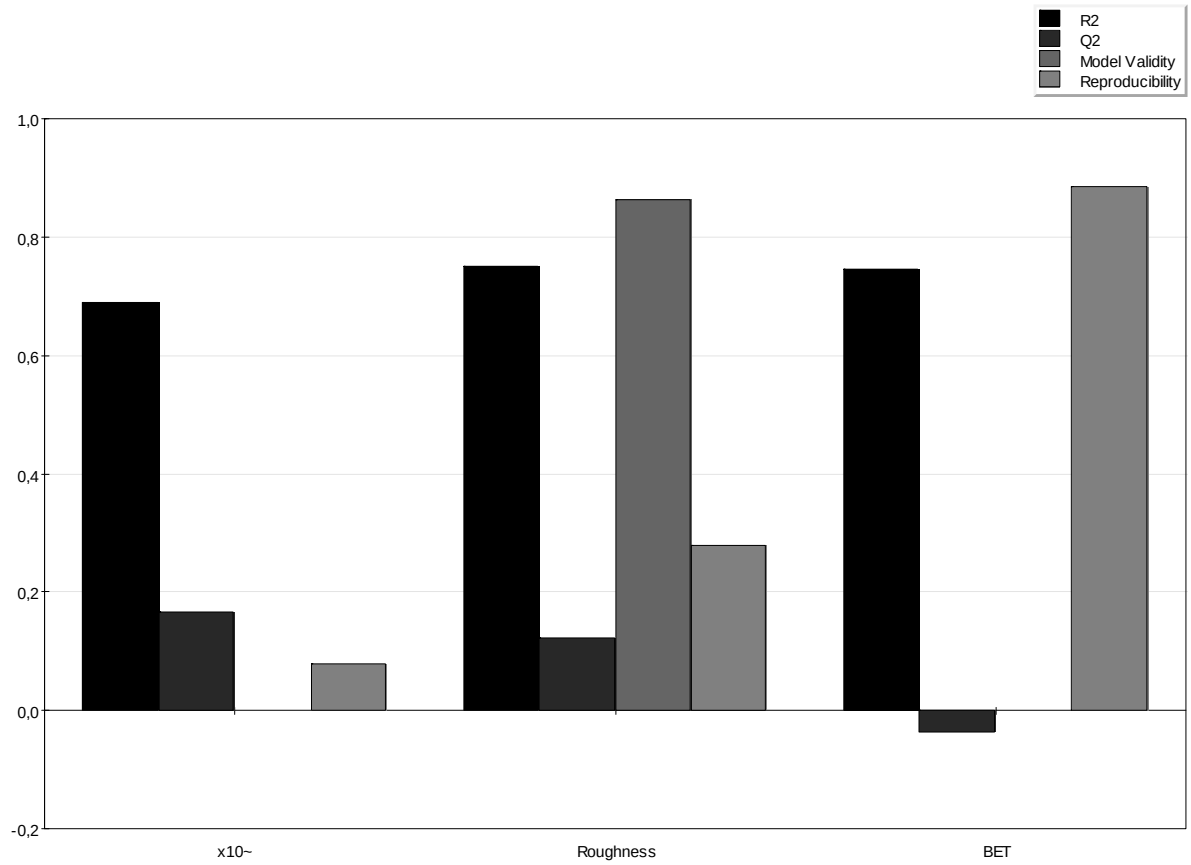

Figure 24: Summary fit; R^2 is goodness of a model fit. It is a measure of how well it is possible to produce current runs. A value of 0.5 stands for a model with a rather low significance. Q^2 is the percent of variation of the response predicted by the model according to cross validation. Q^2 is an indicator of how well the model predicts new data. Q^2 should be greater than 0.1 for a significant model and greater than 0.5 for a good model. Model validity is a test of diverse model problems. A value less than 0.25 indicates statistically significant problems, such as the presence of outliers, an incorrect model, or a transformation problem. The reproducibility is the variation of the response under the same conditions (pure error), often at the center points, compared to the total variation of the response. A reproducibility above 0.85 indicates reproducible experiments. While a reproducibility of <0.5 presents a poor control and a large pure error. The most promising model is marked in red.

In Figure 24 it can be seen that according to R^2, Q^2, Model Validity and Reproducibility the response factor roughness seems to be the most promising one. For the x10 and the BET surface area the summary of fit plot shows that the models do not fit the data well. Therefore the parameter roughness was considered . For the roughness model the R^2 is 0.750 and Q^2 is 0.122, while the model validity has a value of 0.863 and the reproducibility is 0.279. Thus, according to the small Q^2 value the model seems to be invalid. For analyzing the reasons of that, the various parameters calculated with the PLS fit were assessed.

To investigate the variations of the measurements a replicate plot was created (Figure 25).

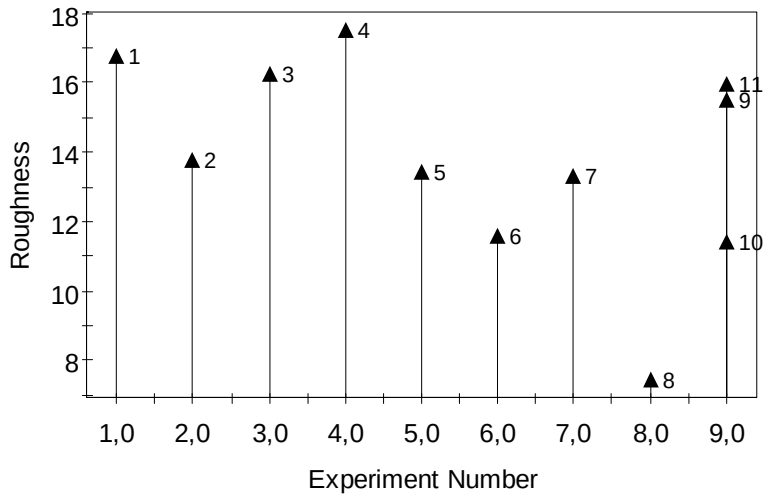

Figure 25: The replicate plot shows the variation in results for all experiments. Repeated experiments appear on the same stick.

The replicate plot represents a graphical version of the “signal to noise – ratio”; in this graph it can be noticed that the centre point measurements from 9 to 11 differ, as experiment 10 seems to be an “outlier”. But the variability of the repeated experiments is still less than the overall variability and close to the centre, and with only three samples is difficult to identify which one of the values is an outlier, from a statistical point of view.

To visualize the distribution of the roughness and to check the need of introducing a transformation of the model, the histogram plot of the data was evaluated (Figure 26).

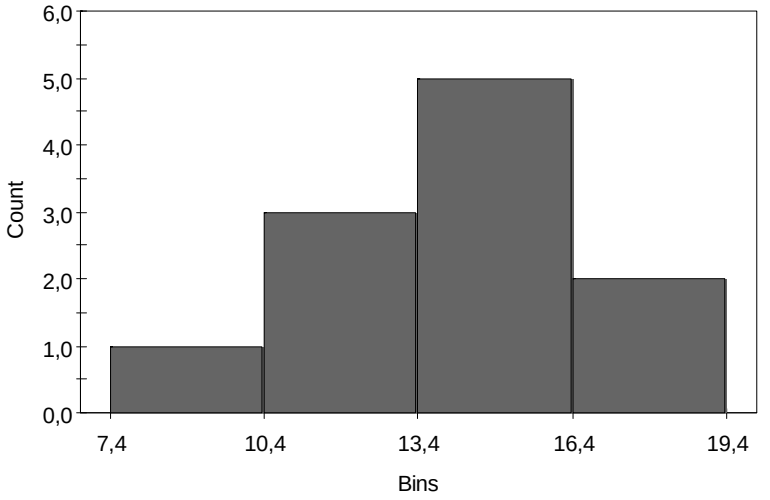

Figure 26: Histogram plot

In Figure 26 it can be observed that the data are normally distributed, which is the desired allocation as, in general, normally distributed responses give a better model estimates and statistics. In a next step the significance of the factors were investigated by analysing a

coefficient plot (Figure 27). The coefficient plot shows the importance of the model terms and therefore, it is very useful for model refinement.

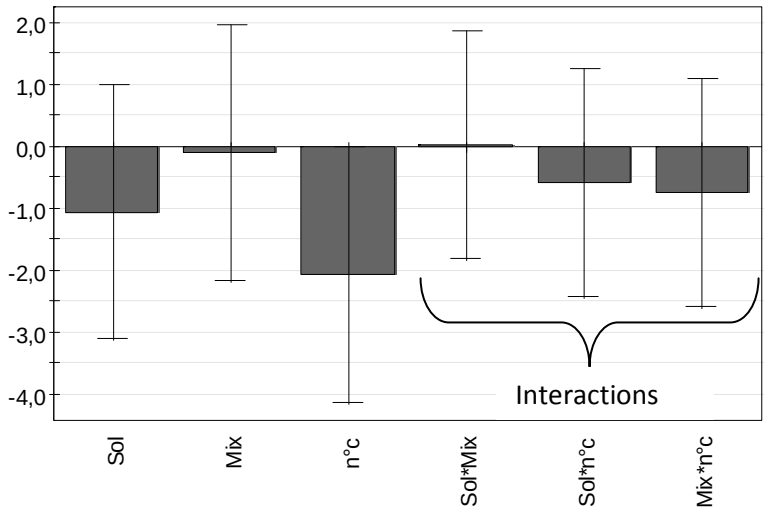

Figure 27: Coefficient plot Roughness. sol indicates the solvent/solid ratio; mix the mixing time; n°c the number of cycles.

According to the coefficient plot for the roughness it can be observed that for the model which includes all factors and interactions, only small and insignificant parameters are associated with the model. This seems to be the reason for the small Q^2 value. Therefore, the model was modified and a new model generated by removing the factors which showed to not have an effect on the roughness. Finally, only the solvent/solid ratio and the number of cycles were included to the analysis (Figure 28), as they were found to affect the roughness.

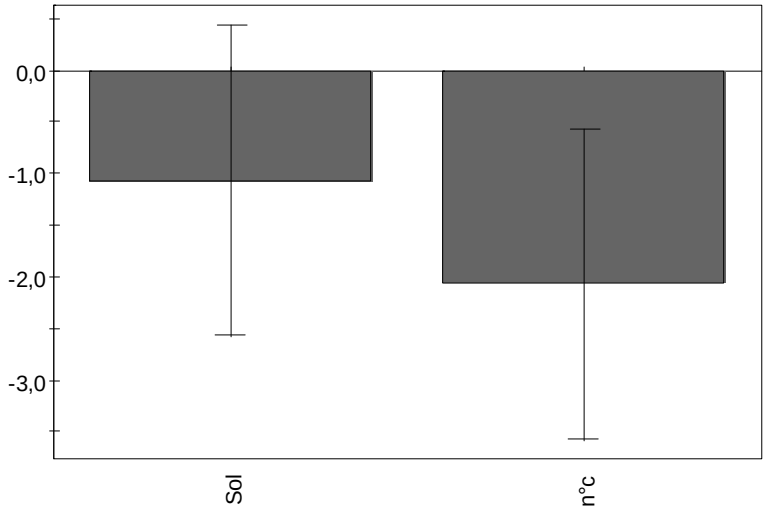

Figure 28: Edited coefficient plot of the response factor roughness. sol indicates the solvent/solid ratio; n°c the number of cycles.

In Figure 28 it can be seen that the number of cycles during the wet decantation process has a significant impact on the roughness of the lactose carrier. Thus, it can be assumed that the higher the number of cycles the smoother the carrier. When increasing the number of cycles one has to consider the increasing costs of solvent. Additionally environmental issues according to disposure of the waste must be taken into account. The golden mean between a good processed product and its costs has to be found.
When removing the interactions and the factor mixing time, a new summary plot was generated (Figure 29).

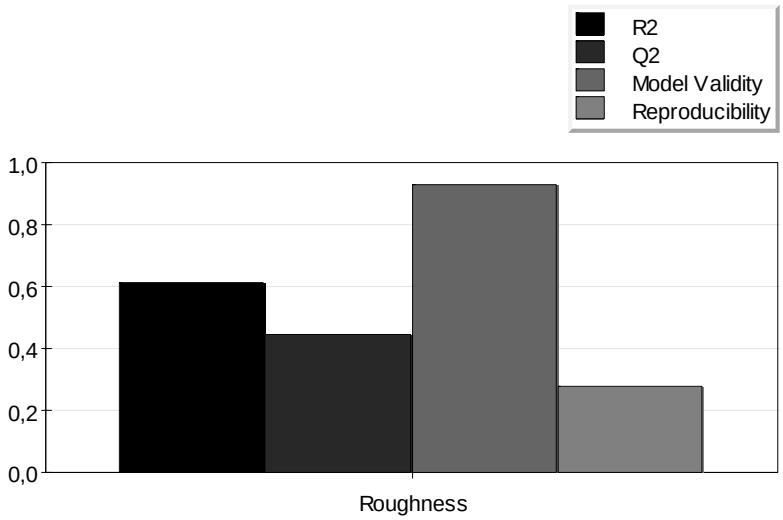

Figure 29: Summary Plot Roughness. R^2 is the goodness of the model fit. Q^2 uncovers how well we can predict new experiments. The model validity is a test of diverse model problems. The reproducibility is the variation of the response under the same conditions (pure error), often at the centre points, compared to the total variation of the response.

After editing the model, R^2 is 0.616 and Q^2 is 0.444. Thus, the Q^2 is increasing while the R^2 is decreasing compared to the first generated model. The model validity has a value of 0.930 and the reproducibility 0.279. In comparison to the original model, the model validity is increasing and the reproducibility remains constant.
Furthermore, the deviation of the model and the measured data is plotted (Figure 30).

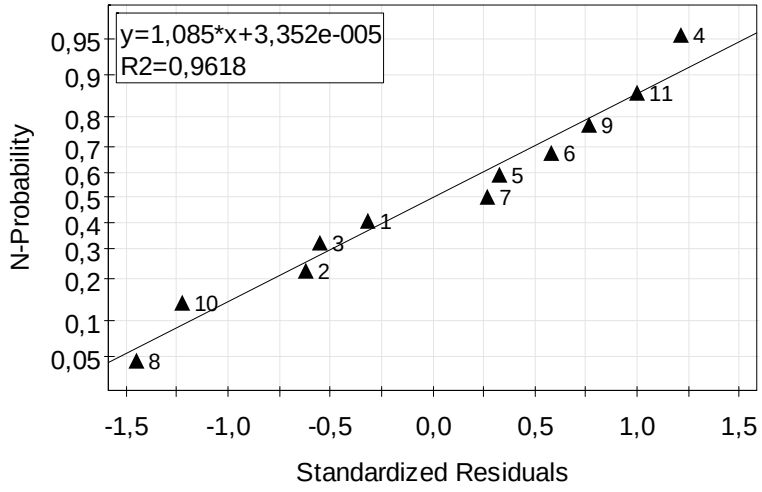

Figure 30: Residual N – plot; the residuals of a response vs. the probability of the distribution of residuals is plotted.

Figure 30 shows the residuals of a response vs. the normal probability (probability of the distribution of residuals) of the distribution. As all points are on a straight line on the diagonal, the residuals are normally distributed noise, which is the ideal result. No deviating experiments can be identified.

Next a plot displaying observed values vs. predicted values was created (Figure 31) to image the relationship between measured and fitted response data. This figure reflects “the model” itself.

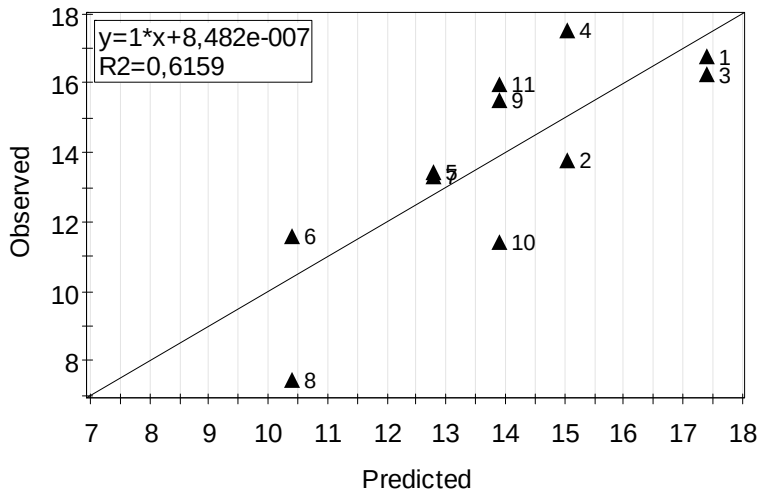

Figure 31: Observed vs. Predicted plot

Figure 31 indicates a good model as the points are relatively close to the line, and a linear relationship was identified. R^2 is 0.616 which reveals an average correlation. Thus, the generated model seems to be applicable for predicting the success of a decantation process.
To summarize the herein presented data: a DOE was performed to study the influence of defined factors (such as: mixing time, number of cycles and solid/solvent ratio) on the wet decantation process. As response factors were chosen the particle size x_{10}, the BET surface area and the roughness of the lactose carrier particles. According to the analysis with MODDE it was observed that a promising model for prediction of the decantation process was obtained only for the roughness of the particles . Here, one significant factor was identified, namely the number of cycles. The higher the number of cycles the smoother the lactose particles after processing. Mixing time and solvent/solid ratio can be excluded in terms of influencing the product performance of a decanted lactose carrier. For a more descriptive model other response factors have to be elected.

4. Conclusion & Outlook

Ensuring development and manufacture of effective, reliable and robust drug products is a major objective of pharmaceutical companies. The performance of carrier-based dry powder inhalation formulations strongly depends on particle interactions between the drug and the carrier. Factors such as particle size and shape, as well as surface properties of the interacting particles, play a decisive role in product performance. Fine lactose particles in the same size range as the API have been found to be a key component in this system of forces to improve the formulation performance. Especially the effect of the carrier smoothness and the role of carrier fines on the *in vitro* deposition of DPI formulations is an important issue.

Herein, a decantation method was applied to remove fine lactose particles from the coarse carrier surface. Therefore, a suitable particle size measurement method was identified in a first step, to prove the removal of fine particles present in the inhalation carrier. Different techniques, laser diffraction and image analysis, as well as different dispersion methods, wet and dry (at various pressures) were tested. It was observed that a wet dispersion method using laser diffraction and applying 20 seconds ultrasound before each measurement provided the best results. Furthermore, a decantation process of 1kg lactose batch was performed to remove the fine particles from the coarse lactose carrier surface. The surface fines were successfully removed by wet decantation, in comparison with the starting carrier material. This was confirmed by SEM images and the thereof calculated surface roughness, as well as particle size measurements. Slight differences in powder attributes of the material before and after decantation were obtained, as observed by the DSC and flowability measurements. No differences between the unprocessed and processed lactose were observed via WAXS and ATR–FT-IR. No changes of the carrier material were observed after storing the carrier at accelerated storage conditions (40 ± 2°C/ 75 ± 5 % RH) for one month.The removal of the fine particles can provide more high energetic spots at the carrier surface which can be occupied with API. This may result in higher adhesion forces between drug and carrier particle. The strong adhesion forces can result in difficulties of drug-particle detachment from the carrier particles during the inhalation process. Therefore, the decanted lactose has to be tested considering these facts, and defined amounts of fines may be added to control these interactions. To improve the decantation process a DoE (Design of experiments) was performed by evaluating critical process parameters (such as: mixing time, solvent/solid ratio and number of cycles) and response factors (particle size x_{10}, roughness, BET surface). After analyzing the data with a PLS (partial least square) regression, it was found that the number of cycles during the wet decantation process proved to significantly affect the process. For further improvement of the model, different factors should be considered in order to investigate how the decantation process can be further improved taking the environmental issues under consideration.

5. References

1. Labiris NR, Dolovich MB. Pulmonary drug delivery. Part I: Physiological factors affecting therapeutic effectiveness of aerosolized medications. Br J Clin Pharmacol. 2003 Aug 20;56(6):588–99.

2. Okamoto H, Todo H, Iida K, Danjo K. Dry Powders for Pulmonary Delivery of Peptides and Proteins. Dry Powders Pulmonary Deliv Pept Proteins. 2002;20(20):71–83.

3. A. S. Chakrabarty, Chakrabarty K. Concepts of pulmonary physiology. In: Cole R, Mackay A, editors. Essentials of respiratory diseasesentials of respiratory disease. 3rd ed. New York: Churchill Livingstone; 1990. p. 49–60.

4. Pilcer G, Amighi K. Formulation strategy and use of excipients in pulmonary drug delivery. Int J Pharm. Elsevier B.V.; 2010 Jun 15;392(1-2):1–19.

5. Islam N, Gladki E. Dry powder inhalers (DPIs) - a review of device reliability and innovation. Int J Pharm. 2008 Aug 6;360(1-2):1–11.

6. Timsina MP, Martin GP, Marriott C, Ganderton D, Yianneskis M. Drug delivery to the respiratory tract using dry powder inhalers. Int J Pharm. 1994;101:1–13.

7. Rita Vanbever, Jeffrey D. Mintzes, Jue Wang, Jacquelyn Nice, Donghao Chen, Richard Batycky, Robert Langer DAE. Formulation and Physical Characterization of Large Porous Particles for Inhalation. Pharm Res. 1999;6(11):1735–42.

8. Hickey A. Pharmaceutical inhalation aerosol technology. 1st ed. New York: Dekker, Marcel; 1992.

9. Marriott C, Frijlink HW. Lactose as a carrier for inhalation products: breathing new life into an old carrier. Preface. Adv Drug Deliv Rev. 2012 Mar 15;64(3):217–9.

10. Zeng XM, Martin a P, Marriott C, Pritchard J. The influence of carrier morphology on drug delivery by dry powder inhalers. Int J Pharm. 2000 Apr 25;200(1):93–106.

11. Kawashima Y, Serigano T, Hino T, Yamamoto H, Takeuchi H. Effect of surface morphology of carrier lactose on dry powder inhalation property of pranlukast hydrate. Int J Pharm. 1998 Oct;172(1-2):179–88.

12. Larhrib H, Zeng XM, Martin GP, Marriott C, Pritchard J. The use of different grades of lactose as a carrier for aerosolised salbutamol sulphate. Int J Pharm. 1999 Nov 25;191(1):1–14.

13. Young PM, Roberts D, Chiou H, Rae W, Chan H-K, Traini D. Composite carriers improve the aerosolisation efficiency of drugs for respiratory delivery. J Aerosol Sci. 2008 Jan;39(1):82–93.

14. Atkins PJ. Dry powder inhalers: an overview. Respir Care. 2005 Oct;50(10):1304–12; discussion 1312.

15. Iida K, Hayakawa Y, Okamoto H, Danjo K, Luenbergerb H. Effect of surface covering of lactose carrier particles on dry powder inhalation properties of salbutamol sulfate. Chem Pharm Bull (Tokyo). 2003 Dec;51(12):1455–7.

16. Boshhiha A, Urbanetz N. Influence of carrier surface fines on dry powder inhalation formulations. Drug Dev Ind Pharm. 2009 Aug;35(8):904–16.

17. Chan LW, Lim LT, Heng PWS. Immobilization of fine particles on lactose carrier by precision coating and its effect on the performance of dry powder formulations. J Pharm Sci. 2003 May;92(5):975–84.

18. Jones MD, Price R. The influence of fine excipient particles on the performance of carrier-based dry powder inhalation formulations. Pharm Res. 2006 Aug;23(8):1665–74.

19. Zeng XM, Martin GP, Tee S-K, Marriott C. The role of fine particle lactose on the dispersion and deaggregation of salbutamol sulphate in an air stream in vitro. Int J Pharm. 1998 Dec;176(1):99–110.

20. Wierik HT, Diepenmaat P, Damhuis R. Formulation of Lactose for Inhaled Delivery Systems. Pharm Technol Eur. 2002;14(11):47–52.

21. Machado JJB, Coutinho JA, Macedo EA. Solid – liquid equilibrium of alpha -lactose in ethanol / water. Fluid Phase Equilib. 2000;173:121–34.

22. Buckton G, Darcy P. Assessment of disorder in crystalline powders - a review of analytical techniques and their application. Int J Pharm. 1999 Mar 15;179(2):141–58.

23. DFE Pharma. Lactose - Some basic properties and characteristics. DFE pharma; p. 1–11.

24. Paul L, Anderson K, Staniforth JN. Protein deposition from dry powder inhaler: Fine particle multiplets as performance modifiers. Pharm Res. 1998;15(4):562–9.

25. Steckel H, Markefka P, TeWierik H, Kammelar R. Functionality testing of inhalation grade lactose. Eur J Pharm Biopharm. 2004 May;57(3):495–505.

6. Kassem NM. Generation of deeply inspirable clouds from dry powder mixtures. University of London; 1990.

27. Rowe RC, Sheskey PJ, Quinn ME, editors. Handbook of pharmaceutical excipients. 6th ed. London, Chicago: Pharmaceutical Press and American Pharmacists Association; 2009.

28. Steckel H, Markefka P, teWierik H, Kammelar R. Effect of milling and sieving on functionality of dry powder inhalation products. Int J Pharm [Internet]. 2006 Feb 17 [cited 2013 Aug 24];309(1-2):51–9.

29. El-Sabawi D, Edge S, Price R, Young PM. Continued investigation into the influence of loaded dose on the performance of dry powder inhalers: surface smoothing effects. Drug Dev Ind Pharm. 2008;32(10):1135–8.

30. Musa R, Bilizi R, Ventura P, Chiesi P. Modified carrier particles for use in dry powder inhalers. 2000.

31. Islam N, Stewart P, Larson I, Hartley P. Lactose surface modification by decantation: are drug-fine lactose ratios the key to better dispersion of salmeterol xinafoate from lactose-interactive mixtures? Pharm Res. 2004 Mar;21(3):492–9.

32. El-Sabawi D, Price R, Edge S, Young PM. Novel temperature controlled surface dissolution of excipient particles for carrier based dry powder inhaler formulations. Drug Dev Ind Pharm. 2006 Feb;32(2):243–51.

33. Freeman RE, Fu X. Characterization of powder bulk, dynmic flow and shear properties in relation to die filling. Powder Technol. 2007;174(1/2):25–33.

34. Glatter O. Small Angle X-ray Scattering. London: Academic Press; 1982.

35. U.S Department of Health and Human Services, Administration, Food and DrugResearch C for DE and, Research C for BE and. Guidance for Industry Q1A (R2) Stability Testing of New Drug Substances and Products. 2003.

36. Umetrics Academy. Chapter 18. Design of experiments.

37. Wold S, Josefson M, Gottfries J, Linusson A. The utility of multivariate design in PLS modeling. J Chemom. 2004 Mar 26;18(34):156–65.

38. U.S Department of Health and Human Services, Food and Drug Administration, Center for Drug Evaluation and Research, Center for Biologics Evaluation and Research. Guidance for Industry Q11 Development and Substances. 2012.

39. HORIBA Instruments. A guidebook to particle size analysis. Irvine, CA; p. 1–30.

40. Podczeck F. Adhesion forces in interactive powder mixtures of a miconized drug and carrier particles of various particle size distributions. J Adhes Sci Technol. 1998;12(12):1323–39.

41. Hogg R. Issues in Particle Size Analysis. KONA Powder Part J. 2008;26(26):81–93.

42. Hassan MS, Lau R. Inhalation performance of pollen-shape carrier in dry powder formulation with different drug mixing ratios: comparison with lactose carrier. Int J Pharm. 2010 Feb 15;386(1-2):6–14.

43. Islam MIU, Langrish T a. G. An investigation into lactose crystallization under high temperature conditions during spray drying. Food Res Int. Elsevier Ltd; 2010 Jan;43(1):46–56.

44. Ferrari F, Cocconi D, Bettini R, Giordano F, Santi P, Tobyn M, et al. The surface roughness of lactose particles can be modulated by wet-smoothing using a high-shear mixer. AAPS PharmSciTech. 2004 Jan;5(4):e60.

45. Jacquot M, De Donato P, Barres O, Pons M., Scher J, Miclo A, et al. Physicochemical characterisation of the lactoperoxidase system powders: comparison of two drying techniques. Powder Technol. 2002 Dec;128(2-3):205–12.

46. Fitzpatrick JJ, Barringer SA, Iqbal T. Flow property measurement of food powders and sensitivity of Jenike's hopper design methodology to the measured values. J Food Eng. 2004;61(3):399–405.

47. Pharmaceutical Technical Procedures, 2.9.16 Flowability. European Pharmacopeia 4. p. 208.

48. Wold S, Eriksson L, Trygg J, Kettaneh N. The PLS method - partial least squares projections to latent structures - and its applications in industrial RDP (Research,Development,and Production). 2004;1:1–44.

49. Eriksson L, Johansson E, Wikström C. Mixture design — design generation, PLS analysis, and model usage. Chemom Intell Lab Syst. 1998;43:1–24.

6. Appendix

6.1 Helos dry dispersion

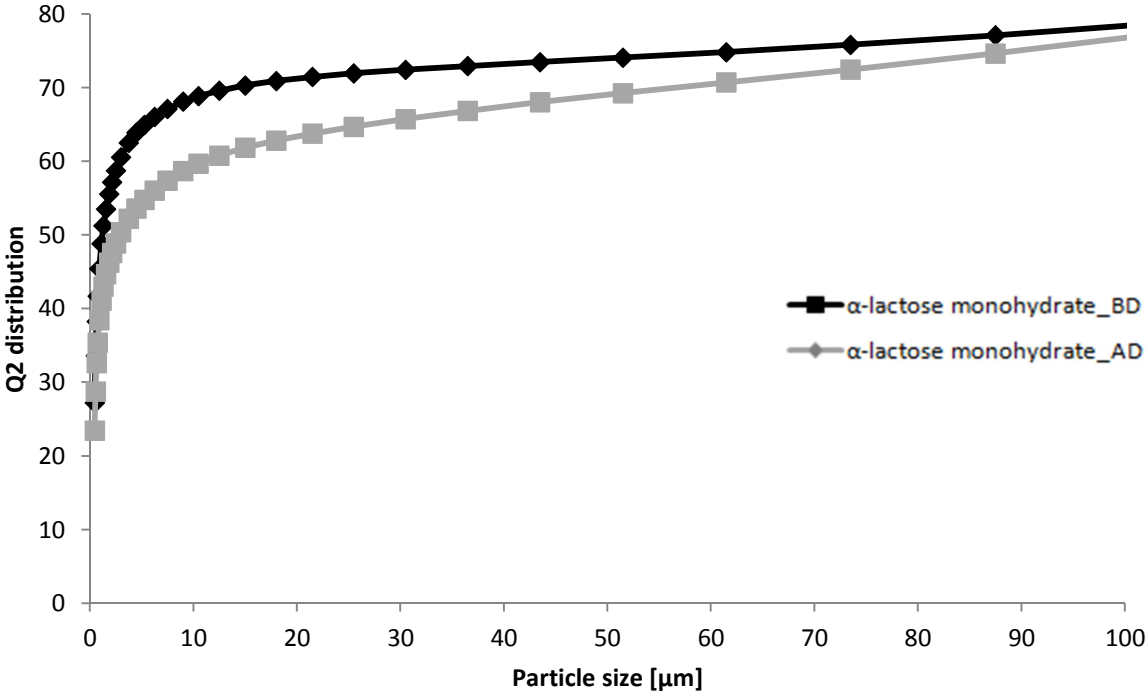

Figure 32: Helos dry dispersion 0.5 bar – Q2 distribution

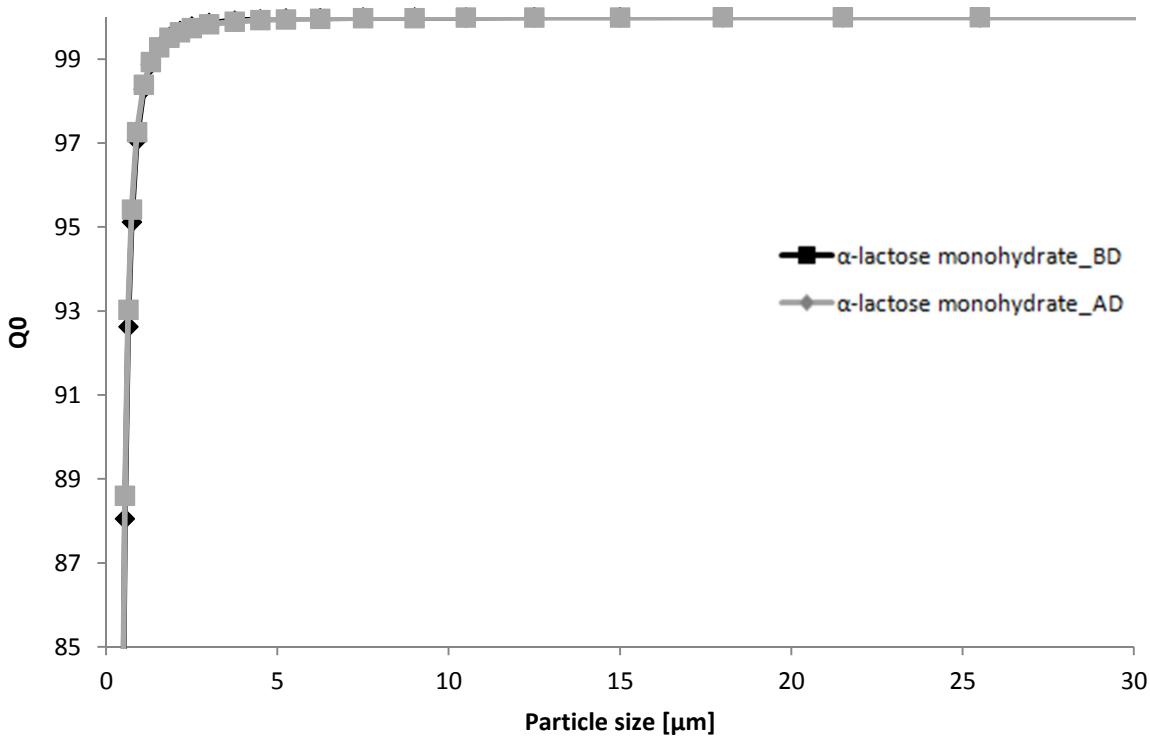

Figure 33: Helos dry dispersion 0.5 bar – Q0 distribution

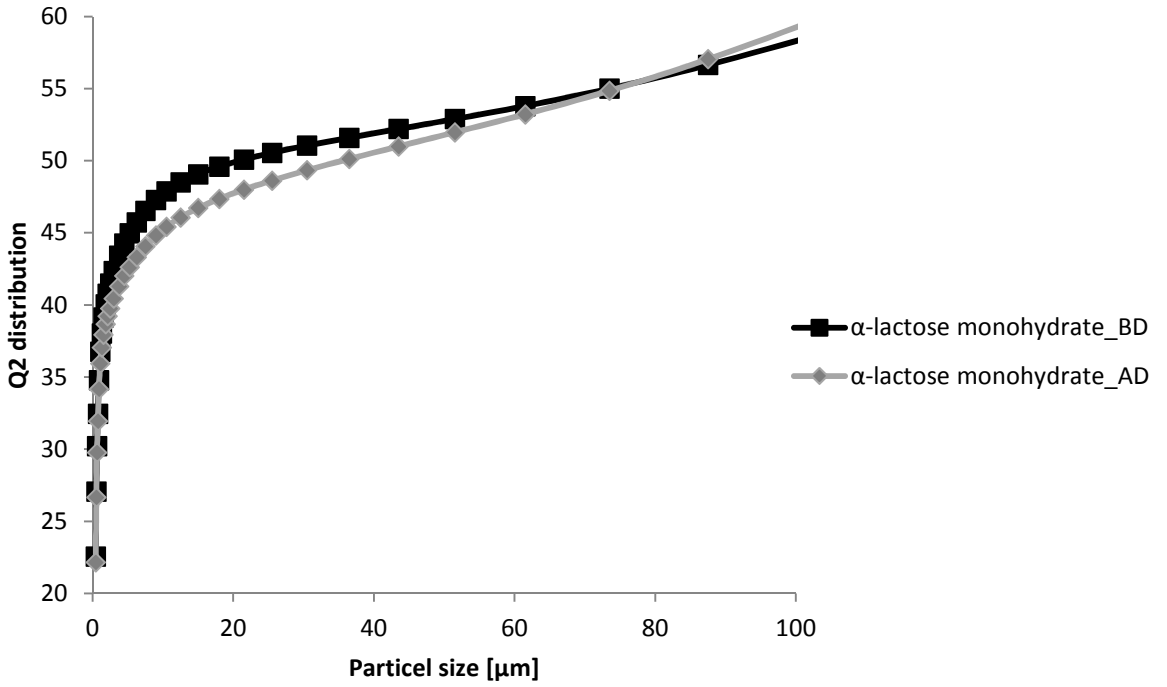

Figure 34: Helos dry dispersion 2.5 bar – Q2 distribution

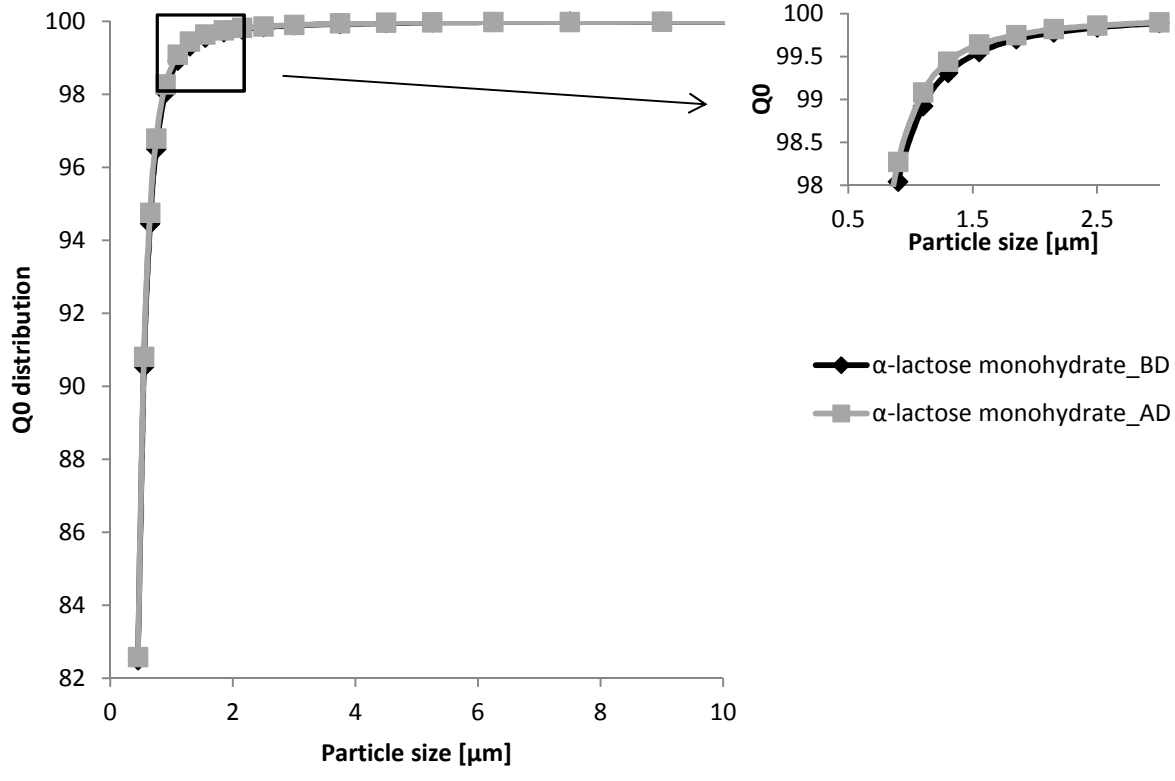

Figure 35: Helos dry dispersion 2.5 bar – Q0 distribution

6.2 Mastersizer dry dispersion

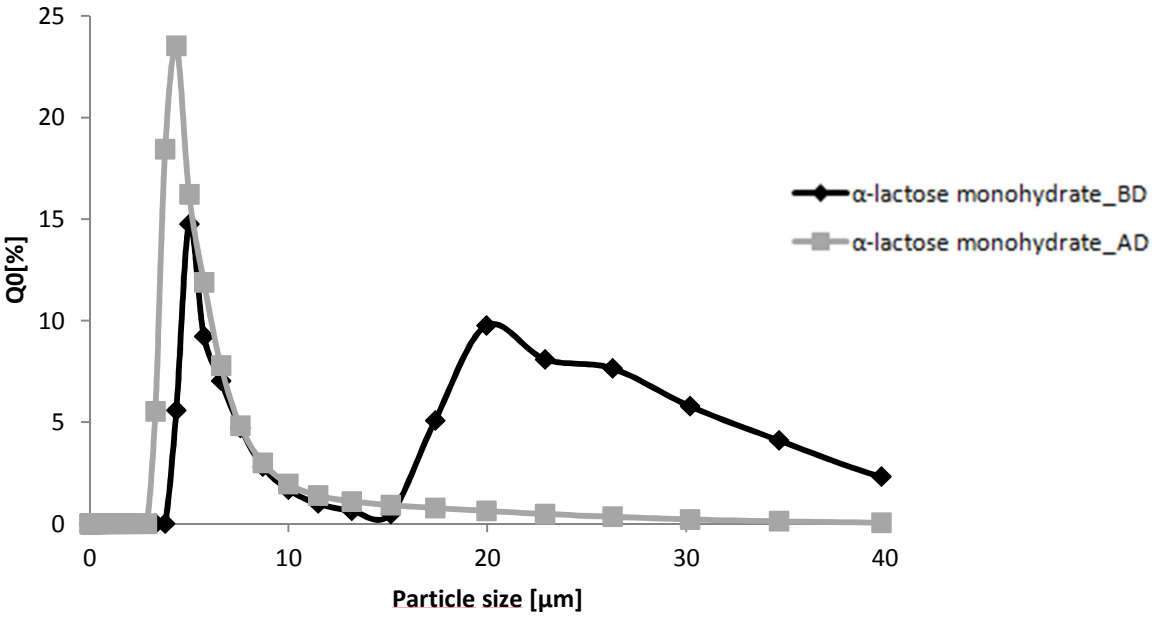

Figure 36: Q0 distribution – Mastersizer (0.5bar)

6.3 Mastersizer wet dispersion

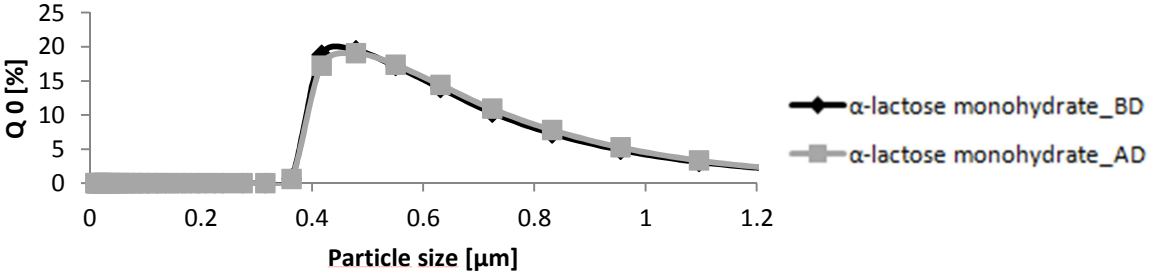

Figure 37: Q0 distribution – Mastersizer wet dispersion – applying 20 sec ultrasound before each measurement